



## **Bakalářská práce**

# **Impacts of textile fibres on environmental microorganisms**

*Studijní program:*

B0719A130001 Nanotechnologie

*Autor práce:*

**Anna Böhmová**

*Vedoucí práce:*

Mgr. Nhung H.A. Nguyen, Ph.D.  
Oddělení aplikované biologie

*Konzultant práce:*

RNDr. Alena Ševců, Ph.D.  
Oddělení aplikované biologie

Liberec 2024



## Zadání bakalářské práce

# Impacts of textile fibres on environmental microorganisms

<i>Jméno a příjmení:</i>	<b>Anna Böhmová</b>
<i>Osobní číslo:</i>	M21000075
<i>Studijní program:</i>	B0719A130001 Nanotechnologie
<i>Zadávající katedra:</i>	Katedra chemie
<i>Akademický rok:</i>	2023/2024

### Zásady pro vypracování:

1. Studying the theory of textile fibres and environmental microorganisms
2. Performing the growth curves of microorganisms
3. Exposing textile fibres on microorganisms
4. Applying methods: Optical Density (OD), Colony Forming Units (CFU), DNA extraction, qPCR for microbial abundance, Observing microbes under fluorescent microscope, Scanning electron microscope (SEM)
5. Evaluating the effects of textile fibres on microorganisms

*Rozsah grafických prací:* dle potřeby dokumentace  
*Rozsah pracovní zprávy:* 50 stran  
*Forma zpracování práce:* tištěná/elektronická  
*Jazyk práce:* angličtina

### **Seznam odborné literatury:**

1. PERIYASAMY, Aravin Prince and TEHRANI-BAGHA, Ali. A review on microplastic emission from textile materials and its reduction techniques. *Polymer Degradation and Stability*. 1 May 2022. Vol. 199, p. 109901. DOI 10.1016/j.polymdegradstab.2022.109901.
2. DE FALCO, Francesca, GULLO, Maria Pia, GENTILE, Gennaro, DI PACE, Emilia, COCCA, Mariacristina, GELABERT, Laura, BROUTA-AGNÉSA, Marolda, ROVIRA, Angels, ESCUDERO, Rosa, VILLALBA, Raquel, MOSSOTTI, Raffaella, MONTARSOLO, Alessio, GAVIGNANO, Sara, TONIN, Claudio and AVELLA, Maurizio. Evaluation of microplastic release caused by textile washing processes of synthetic fabrics. *Environmental Pollution*. 1 May 2018. Vol. 236, p. 916–925. DOI 10.1016/j.envpol.2017.10.057.
3. MANSHOVEN, Saskia, SMEETS, Anse, TENHUNEN-LUNKKA, Anna, MORTENSEN, Lars and MALARCIUC, Christian. *Microplastic pollution from textile consumption in Europe*. . 2022.

*Vedoucí práce:* Mgr. Nhung H.A. Nguyen, Ph.D.  
Oddělení aplikované biologie

*Konzultant práce:* RNDr. Alena Ševců, Ph.D.  
Oddělení aplikované biologie

*Datum zadání práce:* 11. října 2023  
*Předpokládaný termín odevzdání:* 14. května 2024

prof. Ing. Zdeněk Plíva, Ph.D.  
děkan

L.S.

prof. Ing. Josef Šedlbauer, Ph.D.  
garant studijního programu

V Liberci dne 13. listopadu 2023

## Prohlášení

Prohlašuji, že svou bakalářskou práci jsem vypracovala samostatně jako původní dílo s použitím uvedené literatury a na základě konzultací s vedoucím mé bakalářské práce a konzultantem.

Jsem si vědoma toho, že na mou bakalářskou práci se plně vztahuje zákon č. 121/2000 Sb., o právu autorském, zejména § 60 – školní dílo.

Beru na vědomí, že Technická univerzita v Liberci nezasahuje do mých autorských práv užitím mé bakalářské práce pro vnitřní potřebu Technické univerzity v Liberci.

Užiji-li bakalářskou práci nebo poskytnu-li licenci k jejímu využití, jsem si vědoma povinnosti informovat o této skutečnosti Technickou univerzitu v Liberci; v tomto případě má Technická univerzita v Liberci právo ode mne požadovat úhradu nákladů, které vynaložila na vytvoření díla, až do jejich skutečné výše.

Současně čestně prohlašuji, že text elektronické podoby práce vložený do IS/STAG se shoduje s textem tištěné podoby práce.

Beru na vědomí, že má bakalářská práce bude zveřejněna Technickou univerzitou v Liberci v souladu s § 47b zákona č. 111/1998 Sb., o vysokých školách a o změně a doplnění dalších zákonů (zákon o vysokých školách), ve znění pozdějších předpisů.

Jsem si vědoma následků, které podle zákona o vysokých školách mohou vyplývat z porušení tohoto prohlášení.

# Impacts of textile fibres on environmental microorganisms

## Abstract

In recent years, there has been increasing attention on environmental contamination and its ramifications. One of the debated issues is the presence of microfibers (MFs), primarily released from laundering clothes and textiles, which find their way into the environment through wastewater treatment plants (WWTP). This study aims to explore the theory of textile fibers and their interactions with microorganisms, specifically focusing on bacteria found in activated sludge (AS) in a WWTP in Liberec. The objective is to analyze the impact of textile fibers on microorganisms and assess the potential environmental consequences of these interactions.

To achieve these goals, bacteria isolated from AS were exposed to four different types of MFs: Milled Kevlar fibers (kevlar), White milled cotton fibers (cotton), Milled acrylic fibers (PAN) and Milled polyester fibers (PES) for 7 days at concentrations of 10 mg/L and 100 mg/L. The bacterial growth was evaluated using a spectrophotometer to measure optical density (OD<sub>600</sub>), while scanning electron microscopy (SEM) was utilized to determine bacterial attachment to MFs. In the second part of the study, the four MFs were exposed to AS bacterial community at a concentration of 100 mg/L and investigated the interaction using next-generation sequencing (NGS), which determines microbial abundance and taxonomy.

The results indicated that isolated bacteria did not exhibit any negative behavior to four MFs; however, they demonstrated the ability to colonize the surface of textile MFs, potentially forming biofilms. In the second part, cotton MFs showed the most attractive to bacterial abundance compared to others (Kevlar, PES and PAN), particularly *Magnetospirillum*, *Pseudarcobacter*, and the family *Cellvibrionaceae*. Because of cotton is a natural polymer, its environmental impact may differ from that of synthetic MFs. The attachment of bacteria on MFs would present coated MFs leading to harmful human risk. For example, when attached, bacteria possess antibiotic resistance genes and potentially transfer them and spread the antibiotic resistance.

## Keywords

AS bacteria, MFs, AS water, WWTP, kevlar, cotton, polyester, arctylic

## Abstrakt

V posledních letech se čím dál více pozornosti soustředí na kontaminaci životního prostředí a její problematiku. Jedním diskutovaným tématem jsou mikrovlákna (MFs), které jsou hlavně uvolňovány z praní oblečení a textilií. Do životního prostředí se dostávají prostřednictvím čistíren odpadních vod (ČOV). Cílem této práce je studovat teorii textilních vláken a jejich interakce s mikroorganismy, konkrétně se zaměřuje na bakterie z aktivovaném kalu (AS) v ČOV v Liberci. Konkrétně se zaměřujeme na analýzu vlivu textilních vláken na mikroorganismy a hodnocení potenciálních dopadů, které tyto interakce mohou mít na životní prostředí.

Pro dovršení těchto cílů byly použity nejdříve izolované bakterie z AS, které byly vystaveny čtyřem rozdílným MFs: Milled Kevlar fibers (kevlar), White milled cotton fibers (cotton), Milled acrylic fibers (PAN) and Milled poly-ester fibers (PES) po dobu 7 dnů. MFs byly použity v koncentracích 10 mg/L a 100 mg/L. Růst bakterií byl hodnocen pomocí spektrofotometru pro měření optické hustoty (OD600), zatímco skenovací elektronová mikroskopie (SEM) byla použita pro stanovení uchycení bakterií na MFs. Ve druhé části studie byly čtyři MFs, o koncentraci 100 mg/L, vystaveny bakteriím z AS a zkoumala se interakce pomocí sekvenování nové generace (NGS), které určuje početnost a taxonomii mikrobů.

Výsledky ukázaly, že izolované bakterie nevykazovaly žádné negativní chování ke čtyřem MF. Avšak byla prokázána schopnost kolonizovat povrch textilních MFs, čímž mají potenciál tvořit na nich biofilm. V druhé části byla pozorovaná největší druhová hojnost u bavlněných MFs ve srovnání s ostatními (Kevlar, PES a PAN). Jedinečné druhy byly zejména *Magnetospirillum*, *Pseudarcobacter* a čeleď *Cellvibrionaceae*. Vzhledem k tomu, že bavlna je přírodní polymer, může se její vliv na životní prostředí lišit od vlivu syntetických MFs. Uchycení bakterií na MF může vést ke škodlivému vlivu na člověka. Například bakterie mají geny rezistence vůči antibiotikům a po přichycení mají potenciál přenášet a šířit rezistenci vůči antibiotikům.

### Klíčová slova

AS bakterie, MFs, AS voda, ČOV, kevlar, bavlna, polyester, akryl

## Acknowledgements

I would like to express my sincere thanks to all those who contributed to the completion of my bachelor's thesis.

I am grateful to thank Mgr. Nhung Anh Huynh Nguyen, Ph.D. for guiding my thesis and for her indispensable advice, patience and support throughout the process of completing this thesis. Furthermore I would like to thank Alena Shevtsov, Ph.D. who allowed me to work on this study and provided me with important comments for the development of this thesis. Marlita Marlit thank you very much for helping me in the lab with the experiments.

I also thank Ing. Magda Nechanicka, Ph.D. and Jakub Říha, Ph.D. for their help with next-generation sequencing, which was the key to the successful completion of my work. I would like to thank Ing. Martin Stuchlík for his work with FTIR and thank Prof. Ing. Jakub Wiener, Ph.D. for his advice on the theoretical aspects of MFS number determination. I would like to express my gratitude to ChatGPT for assisting with sentence corrections and transcriptions during the writing of this bachelor's thesis.

A big thank also goes to my family and friends who supported me throughout my studies.

## Funding

This diploma work was supported by the Ministry of Education, Youth and Sports of the Czech Republic through the project Textile-derived microplastics in aquatic ecosystems: identification, characterizations, and effect assessment under grant agreement No. LUAUS23054.

# Obsah

<b>1</b>	<b>Introduction</b> .....	<b>15</b>
<b>2</b>	<b>Literature Overview</b> .....	<b>16</b>
2.1	Definition of MFs .....	16
2.2	Pathways of the MFs to the environments.....	20
2.3	Characterization of MFs .....	22
2.4	Bacteria in WWTPs .....	23
<b>3</b>	<b>Materials and Methods</b> .....	<b>25</b>
3.1	MFs.....	25
3.2	Preparation of AS water medium.....	26
3.3	AS bacterial community .....	26
3.4	Isolated AS bacteria .....	26
3.5	Characterization of AS water.....	27
3.6	Epifluorescence microscopy .....	27
3.7	Scanning electron microscope .....	27
3.8	Fourier transform infrared spectroscopy .....	27
3.9	Method of counting the number of FMs.....	28
3.10	Colony-forming unit (CFU).....	28
3.11	Experiment 1: Exposure of isolated bacteria to MFs.....	29
3.12	Experiment 2: Exposure of AS bacterial community to MFs.....	31
3.13	DNA extraction .....	32
3.14	DNA concentration .....	33
3.15	PCR amplification and NGS.....	34
3.16	Data analysis.....	36



<b>4</b>	<b>Results and Discussion</b> .....	<b>37</b>
4.1	Analysis of water .....	37
4.2	Characterization of MFs .....	38
4.3	Growth curve of isolated AS bacteria .....	42
4.4	Exposure of isolated AS bacteria to MFs .....	44
4.4.1	<i>A. bergerei</i> .....	45
4.4.2	<i>R. zopffi</i> .....	47
4.4.3	<i>A. bouvetii</i> .....	49
4.4.4	<i>A. xinjiangensis</i> .....	51
4.5	Exposure of AS bacterial community to MFs.....	53
4.5.1	Extracted DNA concentration .....	53
4.5.2	Next-generation sequencing of 16S rRNA .....	56
<b>5</b>	<b>Conclusion</b> .....	<b>63</b>

## List of Figures

Figure 2.1.1: Definition of the diameter of thread thickness for different structures according to decitex (adapted from Deitex website).....	16
Figure 2.1.2: Sources and pathways of microfibres from industrial wet processing of textiles. Reproduced with permission from (Chan et al., 2023) .....	17
Figure 2.2.1: The pathways of the MFs to the environment from the wastewater treatment plant. (Adapted from Ramasamy et al., 2022) .....	21
Figure 2.3.1: Multiple microplastics detection methods. (Source from Randhawa 2023).....	23
Figure 3.10.1: Workflow of CFU created with BioRender.com.....	29
Figure 3.11.1: Workflow of exposure of isolated bacteria to MFs created with BioRender.com .....	30
Figure 3.11.2: Sampling point of exposure of isolated bacteria to MFs Created with BioRender.com.....	30
Figure 3.12.1: Workflow of exposure of AS bacterial community to MFs Created with BioRender.com.....	31
Figure 3.12.2: Sampling point of exposure of AS bacterial community to MFs Created with BioRender.com.....	31
Figure 3.13.1: FastDNA™ Spin Kit for Soil DNA Extraction Workflow (adopted MP Biomedicals, 2021).....	33
Figure 3.14.1: Qubit assay Workflow (adopted ThermoFisher 2010). .....	34
Figure 3.15.1: Workflow for PCR purification ((adopted from Werner et al., 2022).....	35
Figure 4.2.1: SEM images and bar graph of the fiber diameter distribution for Kevlar .....	38
Figure 4.2.2: SEM images and bar graph of the fiber diameter distribution for cotton .....	38
Figure 4.2.3: SEM images and bar graph of the fiber diameter distribution for PAN.....	38
Figure 4.2.4: SEM images and bar graph of the fiber diameter distribution for PES .....	39
Figure 4.2.5: FTIR spectrum of Kevlar MFs .....	40
Figure 4.2.6: FTIR spectrum of Cotton MFs .....	40
Figure 4.2.7: FTIR spectrum of PAN MFs .....	40
Figure 4.2.8: FTIR spectrum of PES MFs .....	41
Figure 4.3.1: The cell density (OD600) of each isolated bacterial culture after 8 days.....	43

Figure 4.3.2: Determination of the number of viable bacteria per milliliter (CFU/mL): 2 isolated bacterial cultures and MIX after 5 days by CFU .....	43
Figure 4.3.3: Determination of the number of viable bacteria per milliliter (CFU/mL): 2 isolated bacterial cultures after 5 days by CFU .....	44
Figure 4.4.1: The density (OD600) of <i>A. bergerei</i> exposed to MFs of 10 mg/L and 100 mg/L in AS water medium after 6 days. With 10 mg/L, the left Y-axis is for kevlar, the right Y-axis is for cotton, PAN, PES .....	45
Figure 4.4.2: SEM images. The attachment of <i>A. bergerei</i> on MFs .....	46
Figure 4.4.3: Images of living bacteria (green fluorescence) and dead bacteria (red fluorescence) obtained by epifluorescence microscope. <i>A. bergerei</i> with PAN MFs. ....	46
Figure 4.4.4: The density (OD600) of <i>R.zopfii</i> exposed to MFs of 10mg/L and 100mg/L in AS water medium after 7 days. ....	47
Figure 4.4.5: SEM images. The attachment of <i>R.zopfii</i> on MFs .....	48
Figure 4.4.6: Images of living bacteria (green fluorescence) and dead bacteria (red fluorescence) obtained by epifluorescence microscope. <i>R. zopffi</i> with Kevlar MFs .....	48
Figure 4.4.7: The density (OD600) of <i>A. bouvetii</i> exposed to MFs of 10mg/L and 100mg/L in AS water medium after 7 days. ....	49
Figure 4.4.8: SEM images. The attachment of <i>A. bouvetii</i> on MFs .....	50
Figure 4.4.9: Images of living bacteria (green fluorescence) and dead bacteria (red fluorescence) obtained by epifluorescence microscope. <i>A. bouvetii</i> with PES MFs. ....	51
Figure 4.4.10: The density (OD600) of <i>A. xinjiangensis</i> exposed to MFs of 10mg/L and 100mg/L in AS water medium after 7 days. ....	51
Figure 4.4.11: SEM images. The attachment of <i>A. xinjiangensis</i> on MFs .....	52
Figure 4.4.12: Images of living bacteria (green fluorescence) and dead bacteria (red fluorescence) obtained by epifluorescence microscope. <i>A. xinjiangensis</i> with cotton MFs....	52
Figure 4.5.1: Rarecurves at amplicon sequence variants (ASV) level.....	56
Figure 4.5.2: Alpha diversity of control samples day 0, day 8 and samples with MFs after 8 days at ASV level.....	57
Figure 4.5.3: Principal coordinate analysis (PCoA) of Bray-Curtis distances between samples at genus level.....	59
Figure 4.5.4: Taxonomy of bacterial community at genus level.....	61
Figure 4.5.5: Images of living bacteria (green fluorescence) obtained by epifluorescence microscope .....	61

Figure 4.5.6: SEM images. The attachment of the AS community on MFs ..... 62

## List of Table

Table 2.1.1: Occurrence of different types of microplastics in a freshwater environment (adapted from Bhardwaj et al., 2024)..... 18

Table 4.1.1: AS water components presenting A) Sterilized AS water, B)Non-sterilized AS water ..... 37

Table 4.2.1: Number of MFs and weight of MFs in tested concentrations in this study. .... 39

Table 4.5.1: DNA concentration of control samples day 0, day 8; samples with MFs after 8 days measured by Qubit fluorometer. AT: bacteria attached on MFs, FL: free-living bacteria ..... 55

## List of abbreviations

AS	Activated sludge
ASV	Amplicon sequence variant
AT	Attached bacteria on filter pore size 20 µm
ATR-FTIR	Attenuated total reflectance-Fourier transform infrared
BR	Broad range
CFU	Colony forming unit
DNA	Deoxyribonucleic acid
ds	Double stranded
EBPR	Enhanced biological phosphorus removal
ECHA	European Chemicals Agency
EDS	Energy dispersive X-ray spectroscopy
EPS	Expanded polystyrene
EVA	Ethylene–vinyl acetate
FL	free-living bacteria on 0.2 µm
HNO <sub>3</sub>	Nitric acid
HS	High sensitivity
MFs	microfibres
MPs	microplastic
NaCl	Sodium chloride
NGS	Next-generation sequencing
NSW	New South Wales
OD600	Optical density of 600 nm
PA	Polyamide
PAN	Acrylic
PAOs	Polyphosphate-storing organisms
PC	Polycarbonate
PCoA	Principal Coordinates Analysis
PCR	Polymerase chain reaction
PDMS	Polydimethylsiloxane
PE	Polyethylene

PEP	Polyethylene-polypropylene
PES	Polyester
PET	Polyethylene terephthalate
PHA	Polyhydroxyalkanoates
PMMA	Poly (methyl methacrylate)
POM	Polyoxymethylene
PP	Polypropylene
PPS	Protein Precipitation Solution
PS	Polystyrene
PTFE	Polytetrafluoroethylene
PUR	Polyurethane
PVA	Polyvinyl acetate
PVC	Polyvinylchloride
Pyro-GC-MS	Pyrolysis-gas chromatography-mass spectrometry
rRNA	Ribosomal ribonucleic acid
SEM	Scanning electron microscopy
TOC	Total Organic Carbon
UK	United Kingdom
USA	United States of America
WTWs	Water treatment works
WWTP	Wastewater treatment plan

# 1 Introduction

In the context of the growing interest in environmental issues, this bachelor thesis focuses on microfibrils from plastic (MFs). These entities constitute the subset of microplastics (MPs), characterized by the size of less than 5 mm. These MFs are made of both materials natural such as cotton, synthetic as polyester and acrylic. These polymers are used in the textile industry. Hence the source of MFs is clothing and various textiles. MFs are released during manufacturing, shedding during use, and discharged during end-of-life disposal. In particular, the washing of clothes and textiles has the high potential for MFs release. The main route to the environment is via WWTP, whereby they enter wastewater. As WWTP is not designed to remove MFs, they can be found in aquatic environments such as rivers and oceans, as well as in the atmosphere and soil (De Falco et al., 2019; Liu et al., 2022).

Infected MFs presented in wastewater and sludge can adsorb and transport organic pollutants, heavy metals, and pathogenic organisms. The impacts of MPs include not only physical blockage of the digestive tract but also the release of sorbed chemicals and toxic additives and their transport through the food chain to a human body. In addition, MFs serve as a pro-host for bacterial colonies and may represent a potential source for the transfer of antibiotic resistance genes (Rocha-Santos et al., 2022).

This study focuses on the theory of textile fibres and their interaction with microorganisms derived from activated sludge. Two experiment parts were performed. Bacterial growth curves were carried out for four isolated AS bacteria and then exposed to four MFs at two concentrations (10 and 100 mg/L). The bacterial growth was defined by cell density of OD600 and quantification of viable microorganisms by colony forming unit (CFU). In the second experiment four MFs of 100 mg/L were exposed to AS bacterial community. The bacteria-MF interaction was observed by epifluorescence microscopy and determined by 16S rRNA sequencing (NGS). The NGS data was analyzed to determine microbial abundance taxonomy. The MFs were also well characterized by using scanning electron microscopy (SEM) and Fourier-transform infrared spectroscopy (FTIR). These methods and experiments allowed us to study in more detail interactions between textile fibres and microorganisms and to evaluate their impact on the microbial ecosystem.

## 2 Literature Overview

### 2.1 Definition of MFs

Fibrous microplastics or microfibers (MFs) constitute the distinct subset of microplastics (MPs), distinguished by their shapes, dimensions and potential sources of release increasing attention in recent years. MFs encompass the variety of fibers, which may originate from both natural sources and synthetic materials and later are widely employed in the production of textiles and fabrics. According to the European Chemicals Agency (ECHA) in 2020, MFs are defined as MPs that reach the limit length of 15 mm and the diameter is then given by a length-to-diameter ratio greater than 3. Previous studies have primarily focused on investigating FMs with lengths up to 5000  $\mu\text{m}$ . The ECHA suggests that the minimum of two dimensional factors, such as length and diameter, are necessary for the classification and characterization of MPs shape. However, in the textile industry MFs is applied with unit decitex (dtex), which commonly refers to fibers with the fineness of less than 1 dtex corresponding to the linear density of 1 g/10 km. This marking serves as the indicator of the diameter. Typically, MFs with a round cross section and a fineness ranging from 0.3 to 1.0 dtex generally exhibit a diameter of 5–10  $\mu\text{m}$  (Zhang et al., 2021).

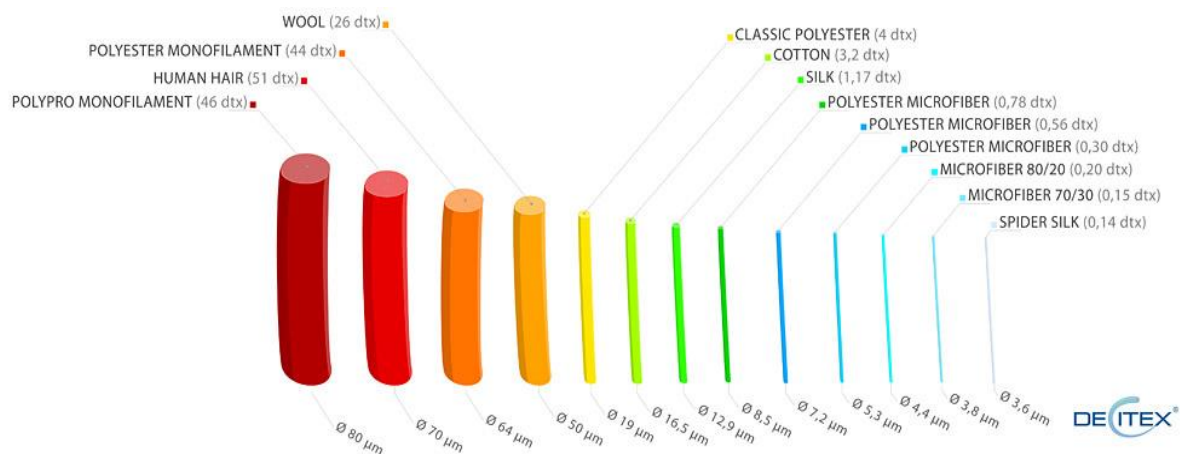


Figure 2.1.1: Definition of the diameter of thread thickness for different structures according to decitex (adapted from Deitex website)

The composition of MFs varies significantly. There are two main categories of fibres found in the environment: natural and synthetic fibres. Natural fibers originate from natural sources and encompass plant-based fibers (cotton, flax, hemp), animal-based fibers (e.g., wool, silk),



and inorganic-based fibers (asbestos). In contrast, synthetic fibers comprise a diverse array of materials produced from synthetic polymers, including polyester (PES), polyamide (PA), polypropylene (PP), and polyacrylic (PAN) (Zhang et al., 2021).

MPs can be distinguished based on their entry into the environment as primary and secondary (Rocha-Santos et al., 2022). Primary MPs originate from various sources such as industrial processes, product wear and tear, such as automotive tires and the release of using synthetic textiles (Syberg et al., 2022). Alternatively, they are intentionally manufactured on a microscale for daily necessities. These include facial cleansers and toothpaste and they artificial microbeads and pellets (with a diameter of approximately 5 mm) or powders (less than 5 mm) used in cosmetic and personal care products. The majority of primary MPs in marine environments consist of fibers released from the production of synthetic textiles and materials. However, classifying them is not always straightforward. For instance, shed fibers from textiles serve as an example how individual studies differ, some designate them as primary, while others classify them as secondary (Zhang et al., 2021).

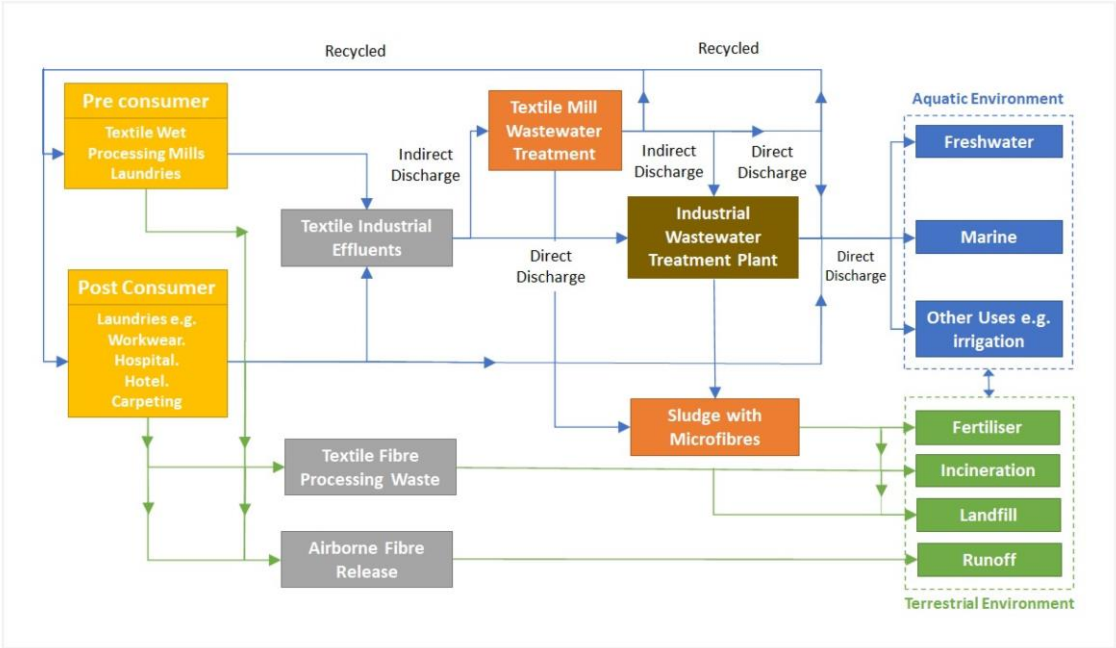


Figure 2.1.2: Sources and pathways of microfibres from industrial wet processing of textiles. Reproduced with permission from (Chan et al., 2023)

Table 2.1.1: Occurrence of different types of microplastics in a freshwater environment (adapted from Bhardwaj et al., 2024)

Locations	Detection methods	Concentration of microplastics	Type/color/size of microplastics	References
Australia	FTIR spectroscopy	1.0 particle/L	PES, PMMA and PA	(Browne et al. <a href="#">2011</a> )
Paris, France	Stereo microscopy	3.0 to 108.0 particles/m <sup>3</sup>	Fibre	(Dris et al. <a href="#">2015</a> )
Switzerland	Visual identification	2.0 × 10 <sup>3</sup> particles/L	Fragments, pellets, cosmetic beads, fibers, films, and foams	(Faure et al. <a href="#">2015</a> )
South Africa	Visual identification	745.4 × 10 <sup>-3</sup> particles/500L	Fragments and fibres	(Naidoo et al. <a href="#">2015</a> )
China	Micro-Raman spectroscopy	100.0 to 4100.0 particles /L	Fibers and granules; PP, PE, PVC and PTFE	(Zhao et al. <a href="#">2015</a> )
USA	Visual identification, FTIR spectroscopy and Raman spectroscopy	0.05 to 32.0 particles/L	Fragments, beads, fibers, films and foam	(Baldwin et al. <a href="#">2016</a> )
Italy	Visual identification and microscopy	0.82 to 4.42 particles/L	Fragments and fibers; PE, PP and PET	(Fischer et al. <a href="#">2016</a> )
China	Micro-FTIR spectroscopy, SEM/EDS	11.0 to 234.6 items/kg in sediment and 3.4 to 25.8 items/L in surface water	Fibers; cellophane, PET, PES and PP	(Su et al. <a href="#">2016</a> )
Northern Tunisia	Stereo microscopy	3000.0 to 18,000.0 items/kg in sediment	Fragments, fibers and pellets	(Abidli et al. <a href="#">2017</a> )
UK	Visual identification, flotation and Raman spectroscopy	660.0 particles/kg in sediment	Fragments and fibers; PP, PES and polyarylsulphone	(Horton et al. <a href="#">2017a</a> )
Amsterdam Canal, Netherlands	Microscopy and FTIR spectroscopy	48.0 to 187.0 particles/L	Fibers and spheres;	(Leslie et al. <a href="#">2017</a> )
Japan	Density separation and FTIR spectroscopy	1900.0 pieces/kg in sediment	PEP, PS, PET, PP, PAN and PE	(Matsuguma et al. <a href="#">2017</a> )
Thailand	Density separation and FTIR spectroscopy	100 pieces/kg in sediment	PEP, PS, PET, PP, PAN and PE	(Matsuguma et al. <a href="#">2017</a> )

USA	Micro-FTIR spectroscopy	0.98 microfibers/L	Cotton, PET, PP, fluoro-polymer/teflon and nitrocellulose/clay	(Miller et al. <a href="#">2017</a> )
China	Stereoscopic microscopy, SEM and FTIR spectroscopy	1660.0 to 8925.0 numbers/L	Fiber; PP and PET	(Wang et al. <a href="#">2017a, b</a> )
Shanghai, China	Density separation, microscopy and micro-FTIR spectroscopy	802.0 items/kg dry weight	Spheres, fibers and fragments; PP, PES, rayon	(Peng et al. <a href="#">2018</a> )
China	Sieving and micro-FTIR spectroscopy	$2.58 \times 10^3$ items/kg in the sediment and 0.330 items/L in the surface water	Fibers, granules and films; PET, cellophane, PE and PVC	(Wang et al. <a href="#">2018</a> )
China	Stereo microscopy and micro-FTIR spectroscopy	0.08 to 7.4 items/L	Fibers; PES, rayon and PP	(Luo et al. <a href="#">2019</a> )
Belgium	Microscopy and spectroscopy		Foam, film, fiber and fragment; EVA, PP, PET, PVC, cellophane, PVA and PA	(Slootmaekers et al. <a href="#">2019</a> )
China	Visual identification, micro-FTIR spectroscopy and GC-MS	0.56 items/L	Foams, films, fragments and fibres; PP, PS, EPS, PVC, PE and PET	(Tan et al. <a href="#">2019</a> )
China	Visual identification, stereomicroscope and micro-Raman spectroscopy	5.0 to 34.0 items/L for surface water and 54.0 to 506.0 items/kg for sediments	Fibers, films, pellets and fragments; PP and PE	(Yuan et al. <a href="#">2019</a> )
UK	FTIR spectroscopy	4.9 particles/L in raw water and 0.00011 particles/L in potable water	PE, PET, PP PS, acrylonitrile and butadiene styrene	(Johnson et al. <a href="#">2020</a> )

## 2.2 Pathways of the MFs to the environments

MFs primarily come from clothing during the laundering process in washing machines (Weis et al., 2022), emerging as a major contributor to MP pollution in WWTPs. Textile production incorporates the wide range of fibers, including natural ones as cotton and wool, synthetic ones as nylon and blends of both such as polyester-cotton. Synthetic fibers as polyester and acrylic have been prevalent in textiles for over 50 years, finding applications in clothing, carpets, upholstery, technical textiles, and various other materials (Napper and Thompson 2016; Weis et al., 2022; Zhang et al., 2011). For example, Browne et al. (2011) found that washing a single garment in a domestic washing machine can release more than 1900 fibers per wash. This process significantly adds to environmental pollution with MPs, especially those derived from synthetic fibers through sewage systems (Napper and Thompson 2016). Other studies have investigated the quantity of MFs released from textiles during a single washing cycle. The release of MFs depends on several factors, such as detergent type, washing program, and textile characteristics (Napper and Thompson, 2016; Weis et al., 2022).

Throughout the lifecycle of synthetic textiles, including production, laundering, usage and disposal, microplastics are released and dispersed into water, air, and soil (Zhang et al., 2021). Wastewater inflowing into WWTP contains all kinds of plastics from households, hospitals and industries. The discharge of treated effluent from WWTPs constitutes the major source of MFs input into aquatic environments. Moreover, the application of sludge and compost serves as a pivotal pathway for the transfer of microplastics to terrestrial ecosystems (Rocha-Santos et al., 2022). While WWTPs can effectively eliminate the majority source of MPs from wastewater (83–99%), the persistent presence of escaping particles and fibers continues to be considered a primary source of environmental contamination. This is mainly due to the high volume of daily discharge. The retention of MPs primarily occurs during sedimentation processes (Rocha-Santos et al., 2022). The barrier provided by wastewater treatment is temporarily circumvented during heavy rainfall events serving as the direct source of MPs in freshwater bodies. MPs exit in WWTP through two primary pathways: direct and indirect. In the direct pathway, microplastics are discharged directly through WWTP effluent carrying significant quantities of microplastics. In the indirect pathway MPs are released from WWTPs into sludge, which is subsequently used as fertilizer in agricultural areas (Bhardwaj et al., 2024).

The WWTP consists of various cleaning stages, which encompass sequential treatment processes including physical, chemical and biological methods (Talvitie et al., 2017). Primary treatment involves mainly mechanical processes including gravity settling, flotation and surface skimming or screening. Certain MFs proceed to the secondary stage, where organic matter is removed through processes such as biodegradation or sorption and entrapment within sewage sludge flocs. This process entails biological treatment, incorporating activated sludge processing (Wu et al., 2022). Most MPs are primarily synthetic (PES, PA, PP, and PAN) and so they are not easily broken down by aerobic or anaerobic bacteria. Those ones intercepted in sewage treatment plants are accumulate in sewage sludge and could be reintroduced into the environment. For instance, if the sludge is applied to land or disposed of in the ocean (Napper and Thompson, 2016). The efficacy of WWTPs in capturing MPs varies depending on the treatment stage under scrutiny (primary, secondary, or tertiary) and the country's regulatory framework (European Environment Agency. 2022) .

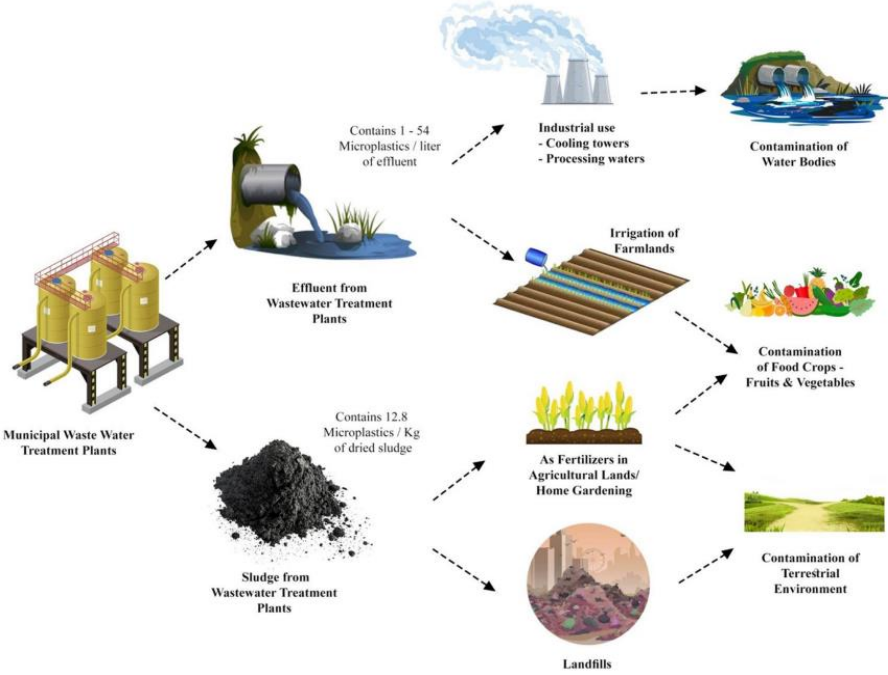


Figure 2.2.1: The pathways of the MFs to the environment from the wastewater treatment plant. (Adapted from Ramasamy et al., 2022)

## 2.3 Characterization of MFs

There are many methodologies used for analyzing MFs those have inherent limitations when they are applied practically. Dependence on only one methodology may yield insufficient data on MPs. Several different analytical techniques are used for completed data of MPs, which work together. (Liza et al., 2024). Various methods are commonly used for the characterization, quantification and identification of microplastics including visual identification; Raman spectroscopy, pyrolysis-gas chromatography-mass spectrometry (Pyro-GC-MS), Fourier-transform infrared spectroscopy (FTIR), scanning electron microscopy (SEM) and combined techniques presenting in Figure 2.3.1: Multiple microplastics detection methods. (Source from Randhawa 2023)

Spectroscopic techniques are reliable and well-established methods used to identify the structure of polymers. They involve matching the emission or absorption spectra of particles with reference spectra. These methods are known for their non-destructive nature and high level of accuracy in identifying the structural properties of polymers. Raman spectroscopy is a suitable method for chemically characterizing MPs in aquatic environments. It generates the molecular fingerprint spectrum based on the polarity of chemical bonds. The sample is exposed to a monochromatic wavelength leading to the generation of a spectrum. This spectrum is subsequently analysed by comparing it with polymer spectral libraries to precisely identify the plastic particles (Bhardwaj et al., 2024). However, one of its primary limitations is the potential degradation of samples due to UV exposure (Silva et al., 2018). FTIR is a widely endorsed method for the chemical analysis of MPs relying on factors such as material composition, configuration and wavelength. Due to the limited spatial resolution of the FTIR spectrum, usually ranging from 10 to 20  $\mu\text{m}$ . This method can only detect microplastics larger than 20  $\mu\text{m}$  restricting its applicability (Liza et al., 2024). SEM and FTIR are widely used techniques for the study of morphology and structural changes during the degradation of MPs (Bhardwaj et al., 2024).

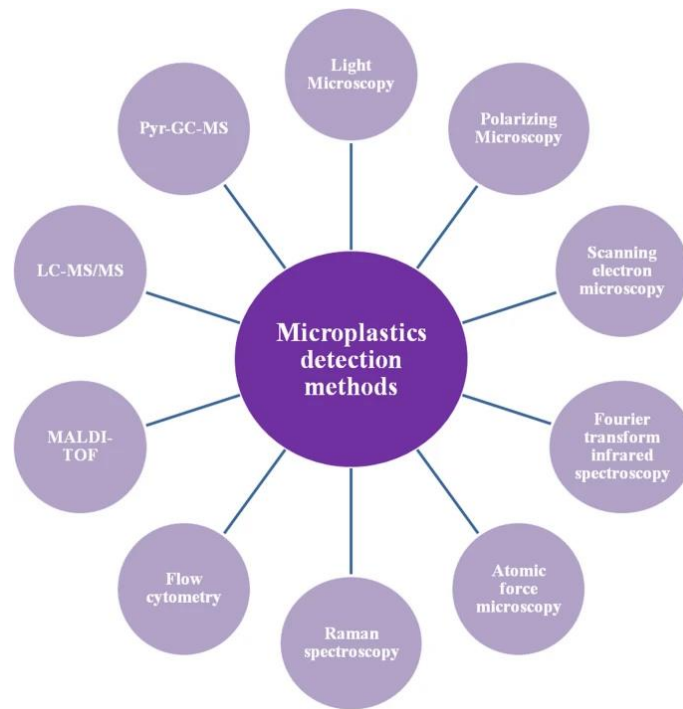


Figure 2.3.1: Multiple microplastics detection methods. (Source from Randhawa 2023)

## 2.4 Bacteria in WWTPs

There can be numerous bacterial communities including pathogens in Wastewater. There are *Enterobacter cloacae*, *Enterococcus faecalis*, *Escherichia coli*, *Klebsiella pneumoniae*, *Proteus vulgaris* and *Pseudomonas aeruginosa*, which can lead to various systemic infections, particularly in individuals with compromised immune systems (Cyprowski et al., 2018). The bacteria play the significant role in the processes of wastewater treatment. This is due to their ability to degrade various organic compounds and cycle elements such as nitrogen, phosphorus and carbon, which is unparalleled in nature (Daims et al., 2006).

The microbial diversity of AS systems can be compared with the ocean microbiome, despite the huge oceans' ecosystem. The majority of the fundamental community members were affiliated with *Proteobacteria*. *Zoogloea* species are suggested as essential agents in denitrification. The microbial community engaged in nitrification, encompassing *Nitrospira* and *Nitrotoga*, has also been identified as a vital taxon emphasizing its importance in nitrite oxidation or complete ammonia oxidation within AS. Two potential polyphosphate-storing organisms (PAOs), *Candidatus Accumulimonas* and *Candidatus Accumulibacter*, were recognized as fundamental taxa in improved enhanced biological phosphorus removal (EBPR) mechanisms. Species from

the *Saprospiraceae* family contribute significantly to the breakdown process in EBPR systems. Temperature plays the critical role in shaping the composition of AS communities. It has a significant impact on the abundance and diversity of slow growing microorganisms such as ammonium-oxidizing bacteria and nitrite-oxidizing bacteria (Wu et al., 2019). In fluctuating environments there is a selection of microorganisms adepted at storing internal compounds like polyphosphate, glycogen and polyhydroxyalkanoates (PHA) as carbon or energy reserves. When organic carbon is presented but other nutrients necessary for microbial growth are temporarily unavailable, most aerobic and anoxic bacteria can store PHA. This PHA stored within biomass can later be extracted as biodegradable polymers suitable for various industrial applications (Ni et al., 2015). The AS from municipal WWTPs holds promise for PHA accumulation (Takabatake et al., 2002).



## 3 Materials and Methods

### 3.1 MFs

This study is focused on 4 four types of fibres from companies Goonvean fibres, kevlar, cotton, polyester (PES) and polyacrylic (PAN) provided within the TEQUATIC project.

Milled Kevlar fibers are classified as synthetic organic polymers. Chemically, they are aromatic polyamides also known as para-aramid. Long-chain synthetic polyamides are manufactured through the spinning of solid fibers using a liquid chemical mixture. The parameters of the fibers are given as the length of 250  $\mu\text{m}$  and the density of 1.44–1.45  $\text{g}/\text{cm}^3$ . They exhibit better mechanical properties compared to steel and glass fibers. These properties make them to be sought after in many applications, such as reinforcement in advanced composites, where their high strength can be utilized. They are high in strength and durability, non-conductive and resistant to abrasion, chemicals and solvents. They have low flammability and do not melt with degradation initiating at temperatures above 400°C. Kevlar fibers are also non-biodegradable (Goonvean Fibres 2024).

White milled cotton fibers are a natural polymer composed of 95 % cellulose. The cellulose is a macromolecule which basic building block is glucose. The microfibers of cotton have the length of 250  $\mu\text{m}$  and a density ranging from 1.48–1.56  $\text{g}/\text{cm}^3$ . These fibers are ideal for the textile industry due to their properties such as breathability, absorbency and good affinity for dyes. They come from the seed pods and are unique for their abilities to retain up to 27 times more water than their weight. They exhibit strong resistance to organic solvents and weak alkalis are biodegradable and flame-retardant and do not melt. Degradation begins at temperatures over 210°C (Goonvean Fibres 2024).

Polyacrylonitrile serves as the basic material for Milled acrylic fibers with the synthetic polymer comprising at least 85% acrylonitrile monomer by weight. These fibers are well-known for their intumescent properties and their role as the chemical precursor to high-quality carbon fibers. Measurements 250  $\mu\text{m}$  in length have the density of 1.17–1.18  $\text{g}/\text{cm}^3$ . They demonstrate significant durability against organic solvents, weak alkalis and acids, their remarkable adaptability and suitability for diverse industrial applications. Their thermal resilience allows operation in high-temperature environments (Goonvean Fibres 2024).

Milled polyester fibers, which are synthetic polymers made of ester functional group compounds, are derived from either fossil fuels or organic sources. Polyester with its length ranging from 250  $\mu\text{m}$  and the density of 1.30–1.40  $\text{g}/\text{cm}^3$  exhibits impressive resistance to acids, most organic solvents, sunlight, weak alkalis, oxidizing agents, stretching and shrinking. These characters make it highly suitable for industrial use. Polyester has the high melting point around 240–260°C. Polyester finds extensive use in consumer goods and industrial applications despite being non-biodegradable, (Goonvean Fibres 2024).

This study uses two concentrations of MFs (10 mg/L and 100 mg/L) exposed to four isolated bacterial cultures and 100 mg/L of MFs exposed to AS bacterial community.

### 3.2 Preparation of AS water medium

The activated sludge (AS) water was collected from WWTP in Liberec located GPS 50.781094, 15.032596. The AS water was passed through a 0.45  $\mu\text{m}$  filter, followed by a 0.2  $\mu\text{m}$  filter with the specific aim of eliminating microbial biomass. Subsequently autoclaving was employed to achieve comprehensive sterilization of the water. It was served as the medium for MFs exposed to isolated bacterial experiments.

### 3.3 AS bacterial community

A part of the collected AS above was set gravity down. The upper part was transferred to a new container to serve as the AS bacterial community for the experiment.

### 3.4 Isolated AS bacteria

Four isolated bacteria: *Algoriella xinjiangensis* (*A. xinjiangensis*), *Glutamicibacter bergerei* (*G. bergerei*), *Acinetobacter bouvetii* (*A. bouvetii*) and *Rhodococcus zophii* (*R. zophii*) with respective accession numbers NR\_145933.1, NR\_025612.1, NR\_117628.1, and NR\_041775.1 were previously isolated in. It was done before the experiment started by researchers in the Department of Applied Biology. The isolated bacteria were maintained on agar plates at 4°C.

### **3.5 Characterization of AS water**

The collected AS water was analyzed as the routine measurement in the Department of Chemistry in CXI, TUL. Total Organic Carbon (TOC) was determined after acidification of the sample with 10 % of phosphoric acid by the combustion method with infrared detection on the TOC Multi N/C 2100S analyzer (AnalytikJena, Germany). Metals were determined after acidification of the sample with concentrated HNO<sub>3</sub> (to pH 2) by plasma spectrometry on the ICP-OES 2100 DV (Perkin Elmer) spectrophotometer. Anions were determined after filtration through the membrane filter with the pore size of 0.45 μm by ion chromatography on the ICS 2100 (IC; ThermoFisher) (Nguyen et al., 2018).

### **3.6 Epifluorescence microscopy**

Fluorescent microscopy enables us to evaluate contamination levels and observes bacterial responses to exposure times with various fibers in the AS water medium. Each sample was initially vortexed to ensure the uniform distribution of microorganisms. Then 2 μL from each sample were placed on a glass slide and combined with 2 μL of Live/Dead fluorescent staining. The resulting microbial mixture was examined with using an Axio Imager fluorescence microscope (Zeiss, Germany).

### **3.7 Scanning electron microscope**

Scanning Electron Microscopy (SEM) is studying morphology and surface features from a micro to nanoscale level. The samples were added in Eppendorf tubes allowing time for the settlement MFs before gently removing the AS water. Then the samples were washed with DI water. A small portion of the samples was transferred onto targets using specially designed carbon tapes. The objective was to identify microorganisms that attach to the MFs. SEM images of the individual textile MFs were also taken to be measured their diameter.

### **3.8 Fourier transform infrared spectroscopy**

Four MFs were analyzed as a measurement in the Department of Chemistry in CXI, TUL. Attenuated total reflection Fourier transform infrared spectroscopy (ATR-FTIR) spectrum was collected within the range of 4000–400 cm<sup>-1</sup>. This was done by the germanium ATR crystal

(NICOLET IZ10, Thermo Scientific, USA) equipped with a single reflection angle  $45^\circ$  horizontal ATR accessory. The resolution was set at  $4\text{ cm}^{-1}$  (Silvestri et al., 2018).

### **3.9 Method of counting the number of FMs**

The procedure for determining the fiber count in one liter of concentrations of 10 mg/L and 100 mg/L involved the following steps. Individual fiber diameters were measured from SEM-acquired images using ImageJ software and subsequently averaged. Manufacturer-provided densities of the textile material were employed. The shape of the fiber was approximated as a cylinder. The volume of the fiber was determined by using the formula for a cylinder based on the diameter and length of the fiber specified by the manufacturer. The density and volume of the textile material were then utilized to derive the mass of a single fiber. Finally, the experimental mass was divided by the calculated mass of one fiber, so that was yielded the fiber count in each sample.

### **3.10 Colony-forming unit (CFU)**

Bacterial colonies described in part 3.4 were grown in the nutrient broth. Then the overnight cultures were centrifuged. The pellets were collected and washed with the physiological solution NaCl 0.9%, then resuspended in the sterilized AS water medium. The bacterial cultures were adjusted to obtain the density of 0.01 using the UV-vis spectrophotometer (Hach Lange DR6000, Germany) with the optical density (OD) of 600. Each bacterium was prepared in triplicate. The total volume of each sample was 15 mL in 20 mL vials. The samples were placed in an incubator with the temperature of  $30^\circ\text{C}$ . Samples were taken after 0, 2, 4, 6, 8, 24, 48, 72, 96, 120, 144, 168 and 192 hours (h) to be measured the cell density by OD600 and the cell growth by colony-forming unit (CFU).

The OD method involves the measurement of the turbidity of bacterial cultures, which is not correlated to the number of bacterial cells. On the other hand, the CFU method provides a direct count of viable bacterial cells by plating dilutions of the culture on agar plates and counting the resulting colonies. By comparing the data obtained from both methods, we can validate the growth curve and assess the accuracy of each technique in monitoring the bacterial growth.

Bacterial turbidity by OD600: 1 mL of each sample was transferred to a clean cuvette and measured by UV-vis spectrophotometer. Deionized water was used as a blank..

CFU: In the flow box each sample was diluted in a 10-fold dilution ranging from  $10^1$  to  $10^6$  with 0.9 % NaCl on agar petri dishes. 100  $\mu$ L of each dilution was pipetted and spread on the surface. Before each step the samples were always vortexed. All agar plates were put into the incubator around 30 °C for 48 hours. CFU were counted and calculated to determine the concentration of bacteria/mL.

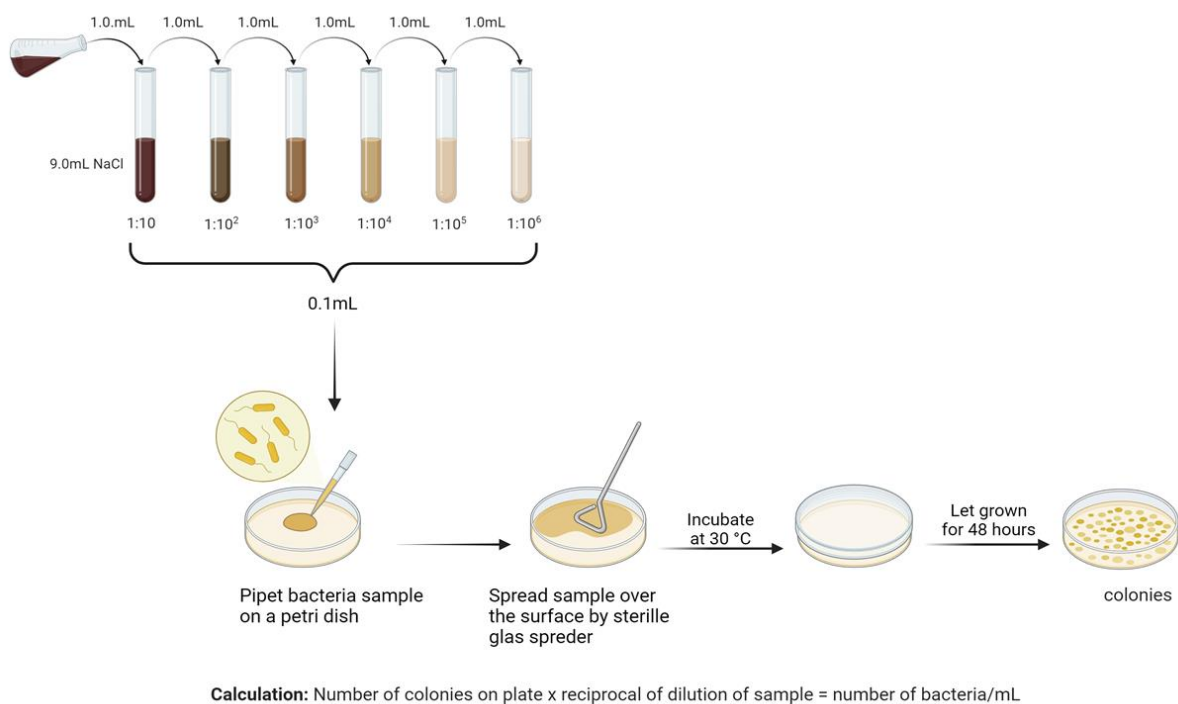


Figure 3.10.1: Workflow of CFU created with BioRender.com

### 3.11 Experiment 1: Exposure of isolated bacteria to MFs

A single colony was taken from each bacterial strain and was cultivated in nutrient broth at the temperature of 26 °C overnight. The cultures were subjected to centrifuged and resuspended into the sterilized AS water. Separately two concentrations (10mg/L and 100mg/L) of four MFs were prepared by mixing them with the sterilized AS water in 50 mL Erlenmeyer flasks. These MFs containing solutions were agitated on a magnetic stirrer from 5 to 10 minutes to ensure homogenous dispersion. Then MFs were sterilized at 120 °C for 30 mins. The bacteria were inoculated into the fiber-enriched medium to achieve a final optical density at 600 nm (OD600) of 0.01. The culture volume was divided into triplicates of 16 mL in vials. The control samples comprising bacteria alone were prepared in triplicate. This experimental protocol was

repeated individually for each bacterial strain. Additionally, the common control samples containing of only MFs in the medium were established for all bacterial strains (Figure 4.2.1).

The triplicate samples were collected for each MFs type. The sampling was conducted after 0, 2, 4 and 7 days post-inoculation. Analytical assessments encompassed fluorescence microscopy for OD600 quantification with subsequent scanning electron microscopy (SEM) analysis performed on terminal samples (Figure 4.2.2).

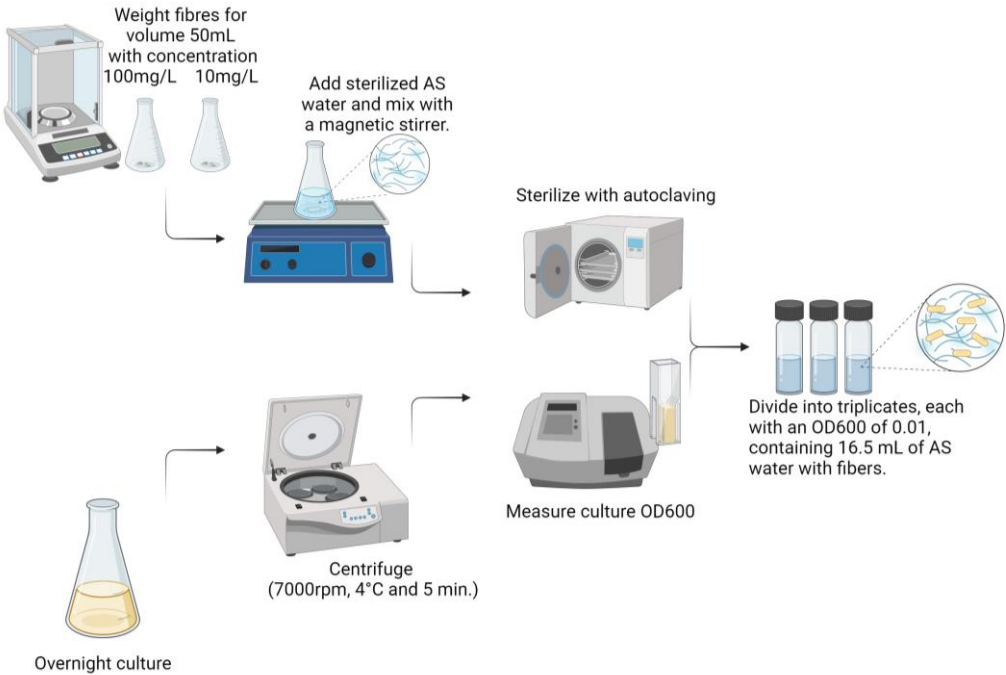


Figure 3.11.1: Workflow of exposure of isolated bacteria to MFs created with BioRender.com

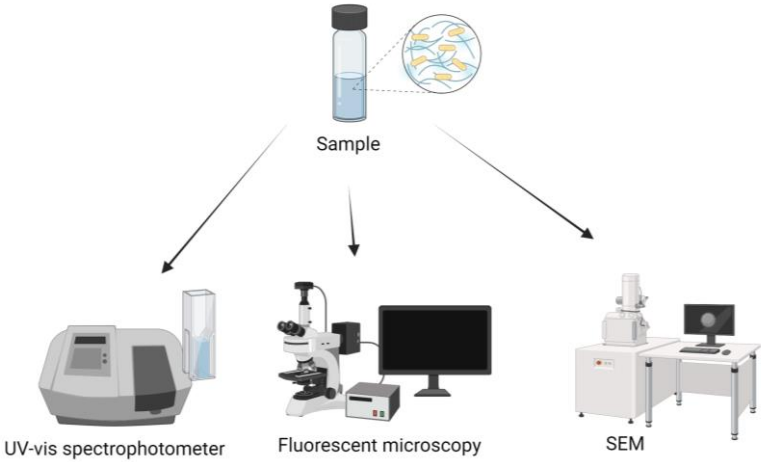


Figure 3.11.2: Sampling point of exposure of isolated bacteria to MFs Created with BioRender.com

### 3.12 Experiment 2: Exposure of AS bacterial community to MFs

MFs from part 3.1 were sterilized within Erlenmeyer flasks containing AS water using autoclaving techniques with a targeted concentration of 100 mg/L per 100 mL. Upon completion of the sterilization procedure, 100 mL of AS water containing the microbiome was introduced into each flask. This was followed by agitation on the magnetic stirrer to ensure a homogeneous distribution of the MFs. These procedures were carefully executed in the triplicates to uphold the reliability and consistency of the results (Figure 4.3.1).

The control sample day 0 was collected in quadruplicate, each 100 mL was passed through 0.2  $\mu\text{m}$  filters for the DNA extraction. After day 8<sup>th</sup> of the experiment all samples were added to filtration through a 20 – 25  $\mu\text{m}$  filter for DNA isolation of bacteria attached on MFs (AT). The filtrated water was continuously passed through a 0.2  $\mu\text{m}$  filter to obtain free-living bacteria (FL). Samples collected on filter papers were carefully transferred into 1.5 mL Eppendorf tubes and stored at  $-80\text{ }^{\circ}\text{C}$ , ensuring optimal preservation of sample integrity for subsequent analytical procedures (Figure 4.3.2).

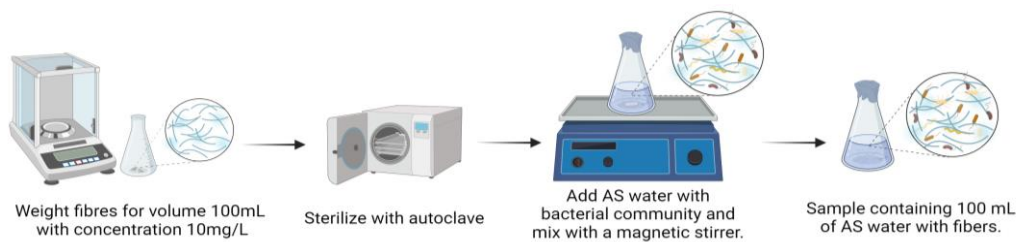


Figure 3.12.1: Workflow of exposure of AS bacterial community to MFs Created with BioRender.com

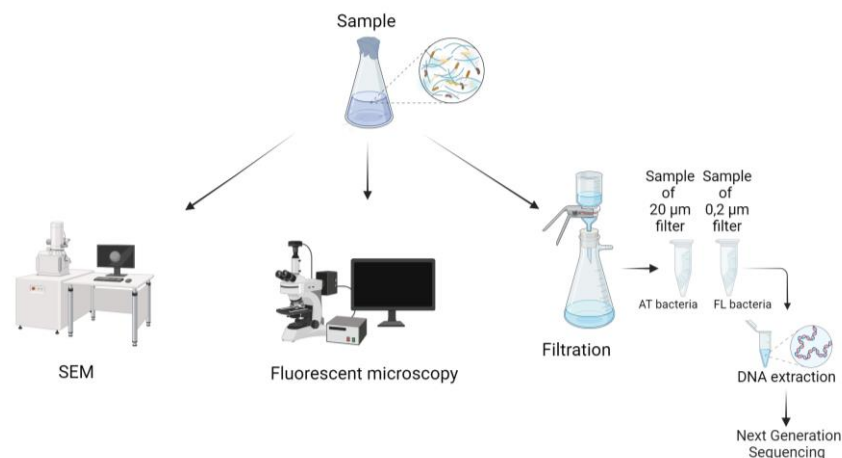


Figure 3.12.2: Sampling point of exposure of AS bacterial community to MFs Created with BioRender.com

### 3.13 DNA extraction

The FastDNA Spin Kit for Soil was used according to the protocol (Figure 3.12.2) to extract DNA from samples collected in part 3.12. This kit is highly efficient due to the FastPrep instrument and Lysing Matrix E tubes, which are designed to efficiently lyse all microorganisms. It can be applied to a large number of environmental samples including bacterial, fungal, plant and animal genomic DNA. The extracted DNA is then purified using a silica-based spin filter method and is suitable for PCR analysis and other downstream applications.

The protocol from The FastDNA Spin Kit for Soil was taken for the procedure. Our samples were in the form of biomass of microorganisms on filters. There were several modifications in the protocol to facilitate or enhance efficiency. In the third step the sample with 250  $\mu\text{L}$  of PPS was not vortexed but only inverted. In the step named “ Bind the DNA”, 600  $\mu\text{L}$  of DNA solution is repeatedly transferred until the entire volume is centrifuged. Between steps 7 and 8 the samples were placed in the heating block of 55  $^{\circ}\text{C}$  for 5 minutes. After the step 8 the extracted samples were stored at the temperature of 4 $^{\circ}\text{C}$  (MP Biomedicals,2021).





Figure 3.13.1: FastDNA™ Spin Kit for Soil DNA Extraction Workflow (adopted MP Biomedicals, 2021)

### 3.14 DNA concentration

The Qubit 2.0 fluorometer was used for measurement the DNA concentration in the samples according to the Qubit assay. Different buffers were applied based on the samples. Our samples contained DNA and were assumed to have a relatively larger quantity, the Qubit dsDNA broad range (BR) buffer was utilized. For one sample 199  $\mu$ L of Qubit BR buffer were prepared with 1  $\mu$ L of Qubit reagent, such as a fluorescent dye, to create the working solution. The amount of working solution was prepared for all samples plus two samples of known DNA concentration to create the standard curve. The 10  $\mu$ L of DNA with a known concentration was introduced

into the standard tubes, while 3  $\mu\text{L}$  of the samples were added to the remaining tubes. After mixing each tube with vortexing they were centrifuged and then incubated at the room temperature and in the dark condition for 2 minutes. The DNA concentration was measured by the Qubit 2.0 fluorometer (ThermoFisher 2021).

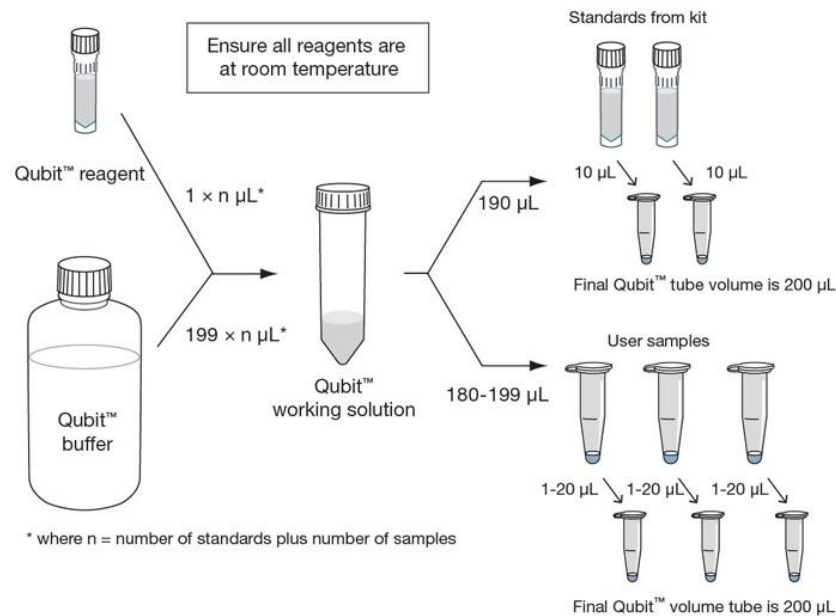


Figure 3.14.1: Qubit assay Workflow (adopted ThermoFisher 2010).

### 3.15 PCR amplification and NGS

The Next-generation sequencing (NGS) process can be divided into three main steps: library preparation, sequencing, and analysis. We utilize primer pairs for sequencing the 16S rRNA gene with a targeted region of V4 to analyze microbial communities in samples. The 16S rRNA gene, approximately 400 bp in length, consists forward primer 515F (5'-TGCCAGCMGCNGCGG-3')<sup>47</sup> and reverse primer 802R (5'-TACNVGGGTATCTAATCC-3'). The initial stage involved constructing a library, which comprised four steps to prepare the samples for sequencing. The process started with the first PCR to amplify the 16S rDNA region. Each reaction was prepared a mixture consisting of 4.5  $\mu\text{L}$  of PCR water, 1  $\mu\text{L}$  of Enhancer, 0.5  $\mu\text{L}$  of 10 $\mu\text{M}$  16S IT-F, 0.5  $\mu\text{L}$  of 10 $\mu\text{M}$  16S IT-R, and 7.5  $\mu\text{L}$  of Kapa HiFi Master. Subsequently 14  $\mu\text{L}$  of the mixture and 1  $\mu\text{L}$  of DNA were pipetted into 200  $\mu\text{L}$  tube strips. All samples were vortexed, centrifuged and underwent PCR. Specific parameters were established for the PCR process: 95  $^{\circ}\text{C}$  – 3 min, 10x: 98  $^{\circ}\text{C}$  – 20 s, 50  $^{\circ}\text{C}$  – 15 s, 72  $^{\circ}\text{C}$  – 30 s and 72  $^{\circ}\text{C}$  – 1 min.

For the second PCR, we labeled the samples with barcodes, which serve as unique identifiers for individual samples. The barcodes are short specific nucleotide sequences attached to one of the primers. We added 3  $\mu\text{L}$  of the primer and barcode mixture and 4  $\mu\text{L}$  of DNA from the first PCR template to the second PCR Mix, comprising 17  $\mu\text{L}$  of PCR water, 1  $\mu\text{L}$  of Enhancer, and 25  $\mu\text{L}$  of Kapa HiFi. After vortexing and centrifugation, the samples were loaded into the PCR machine and the parameters were adjusted according to : 95  $^{\circ}\text{C}$  – 3 min, 35x: 98  $^{\circ}\text{C}$  – 20 s, 50  $^{\circ}\text{C}$  – 15 s, 72 $^{\circ}\text{C}$  – 30 s, and 72 $^{\circ}\text{C}$  – 1 min.

The DNA purification step came then. We combined 50  $\mu\text{L}$  of Agencourt AMPure XP with the entire volume of product from the 2nd PCR, and the mixture was pipetted 10 times to ensure proper binding of the DNA to the magnetic particles. After a 5 minute incubation at room temperature the samples were transferred to a magnetic stand to allow the iron particles settle. When the supernatant was clear, it was pipetted out and 200  $\mu\text{L}$  of 70 % ethanol was added to the tubes. The tubes were rotated about 180 $^{\circ}$  on the magnetic stand six times to ensure proper DNA purification and the ethanol was carefully removed. This process was repeated once more with the addition of 70 % ethanol. The ethanol was completely removed and the samples were incubated for 5 minutes to allow the ethanol evaporate fully. The samples were taken off the magnetic stand, 40  $\mu\text{L}$  of Nuclease-free Water was added and the entire volume was pipetted 10 times. The samples were incubated on the magnetic stand for 2 minutes. The resulting supernatants were stored in the 0.5 mL tubes at 4  $^{\circ}\text{C}$ . Finally, we measured the DNA concentration using the Qubit 2.0.

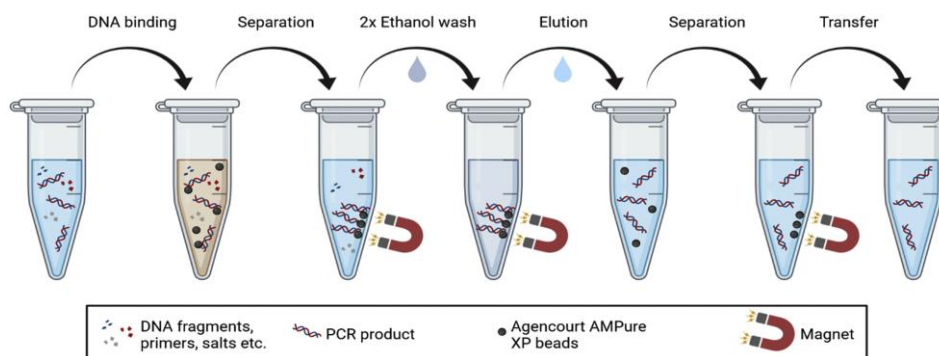


Figure 3.15.1: Workflow for PCR purification (adopted from Werner et al., 2022)

The final step of preparation involves the dilution and library creation. A control sample or MOCK was included. MOCK was the pre-prepared local sample containing of known bacterial genomes of known concentration. The purified PCR products were diluted to the concentration of 5.5  $\text{ng}/\mu\text{L}$ , typically represented as the 25 nM solution in 20  $\mu\text{L}$ . All components were combined into one tube starting with the calculated amount of Nuclease-

free Water and followed by the gradual addition of the calculated amounts of DNA samples and MOCK for this dilution.

The DNA concentration was measured with Qubit dsDNA high sensitivity (HS) buffer before sending the sample for sequencing and analysis. Based on the measured concentration the mixture was diluted with Nuclease-free water to the concentration of 1 nM in a volume of 1 mL. The 1 nM solution was further diluted to the 200–300 pM solution in a volume of 100  $\mu$ L. Sequencing was performed on the Ion Torrent Genexus platform. The DNA sequencing was processed on the Ion Torrent Genexus platform. The procedure was carried out according to the protocol in the laboratory of the Department of Applied Biology.

### **3.16 Data analysis**

The obtained data were processed with QIIME 2 2023.2 software (Bolyen et al., 2019). First, the raw sequence data was demultiplexed and quality-filtered using the q2-demux plugin. Then, denoising was performed with DADA2 (via q2-dada2) (Callahan et al., 2016). Taxonomy was assigned to ASVs (Amplicon Sequence Variant) using the q2-feature-classifier (Bokulich et al., 2018), and classified by classify-sklearn naive Bayes against the Silva 138 database (Quast et al., 2013) and then mitochondria and chloroplast were removed from the dataset. The accuracy of classification was evaluated against an artificial MOCK community sample.

QIIME 2 outputs were processed using the phyloseq R package (McMurdie and Holmes, 2013). The alpha diversity metrics (Observed, Shannon, Simpson and Inverse Simpson) were computed on data rarefied (sub-sampled without replacement) to 29955 sequences per sample. Principal Coordinates Analysis (PCoA) was used to compare bacterial communities across various samples. The Bray-Curtis distance metric was employed to measure the differences between the communities based on their relative abundances without any rarefaction. Additionally, taxonomy bubble plots were created using the same relative abundances but only including bacteria with a mean relative abundance greater than 0.01.

## 4 Results and Discussion

### 4.1 Analysis of water

The outcomes derived from water analysis employing methodologies for metal determination, total organic carbon assessment and an anion identification offering significant findings concerning water quality and its potential influence on bacterial proliferation. Certain metals and organic compounds can serve as sustenance and foster bacterial growth. The anion analysis results unveil the presence of inorganic ions such as chlorides, sulfates, and nitrates, which could impact the bacterial habitat (Zhu et al., 2018).

*Table 4.1.1: AS water components presenting A) Sterilized AS water, B) Non-sterilized AS water*

A: Sterilized AS water		
pH	8,4	
Mg	8.5	mg/l
Ca	75.3	mg/l
Na	164	mg/l
K	36.8	mg/l
Fe	0.11	mg/l
Mn	0.083	mg/l
Cr	0.017	mg/l
Al	0.04	mg/l
Be	< 0.0002	mg/l
Cu	0.014	mg/l
Ag	0.019	mg/l
Ptot	5.47	mg/l
Cl	241	mg/l
SO4	112	mg/l
NO3	63.1	mg/l
NO2	< 0.5	mg/l
NH4	1.93	mg/l
TOC	155	mg/l
TN	40.7	mg/l

B. Non-sterilized AS water		
pH	7,6	
B	0.12	mg/l
Mg	10.7	mg/l
Ca	61.3	mg/l
Na	131	mg/l
K	24.6	mg/l
Fe	0.06	mg/l
Mn	0.009	mg/l
Cr	< 0.005	mg/l
Al	0.03	mg/l
Be	< 0.0002	mg/l
Cu	< 0.05	mg/l
Ag	< 0.005	mg/l
P	7.55	mg/l
Cl	192	mg/l
SO4	89.2	mg/l
NO3	14.9	mg/l
NO2	4.6	mg/l
NH4	8.40	mg/l
PO4	21.6	mg/l
TOC	11.0	mg/l
TN	11.2	mg/l

## 4.2 Characterization of MFs

### MFs morphologies and sizes by SEM

MFs of Kevlar, Cotton, PAN, and PES were observed morphologies using SEM and measured diameters.

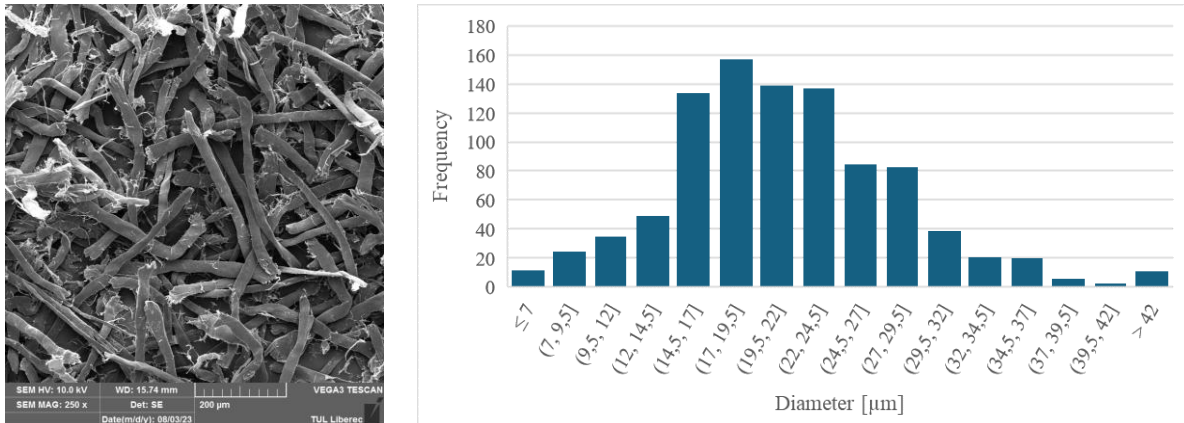


Figure 4.2.1: SEM images and bar graph of the fiber diameter distribution for Kevlar

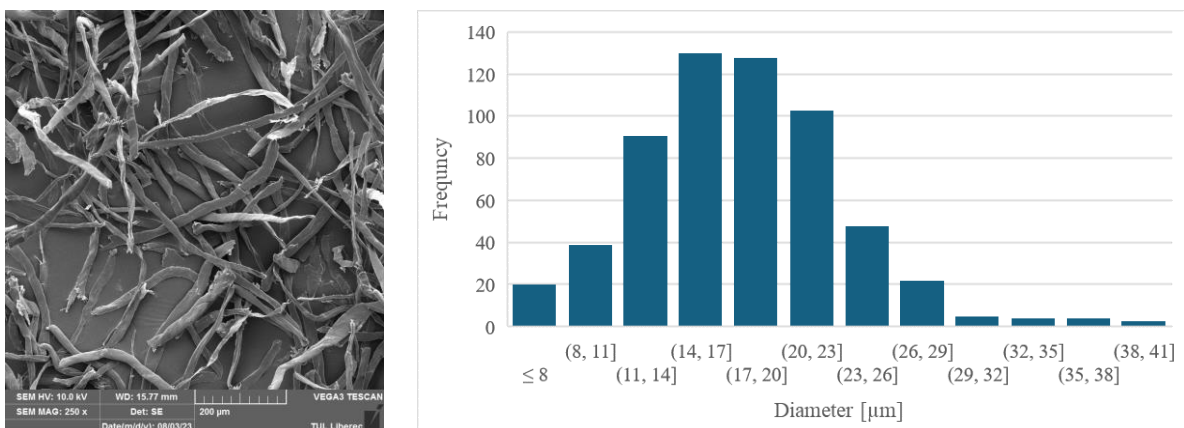


Figure 4.2.2: SEM images and bar graph of the fiber diameter distribution for cotton

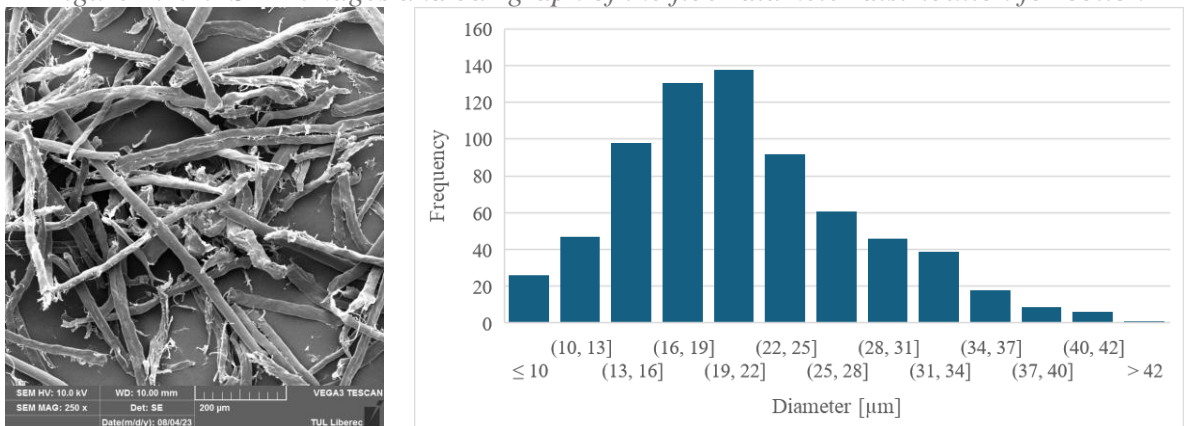


Figure 4.2.3: SEM images and bar graph of the fiber diameter distribution for PAN

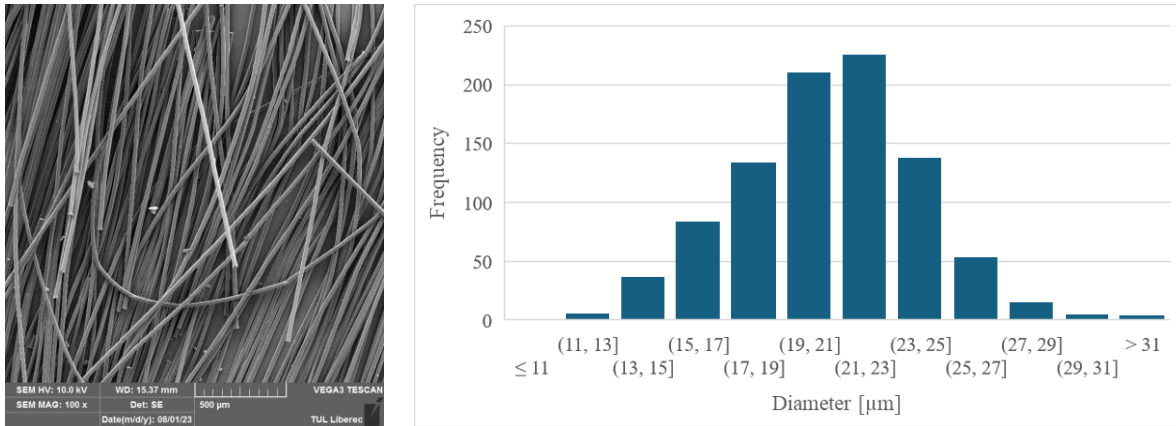


Figure 4.2.4: SEM images and bar graph of the fiber diameter distribution for PES

Table 4.2.1: Number of MFs and weight of MFs in tested concentrations in this study.

Concentration of MFs	Kevlar	Cotton	PAN	PES
10 mg/L	$7.85 \times 10^4$	$1.07 \times 10^5$	$9.78 \times 10^4$	$8.60 \times 10^4$
100 mg/L	$7.85 \times 10^5$	$1.07 \times 10^6$	$9.78 \times 10^5$	$8.60 \times 10^5$
The weight of a single MF [mg]	$1.27 \times 10^{-4}$	$9.36 \times 10^{-5}$	$1.02 \times 10^{-4}$	$1.16 \times 10^{-4}$

Kevlar was exhibited the highest frequency of MFs diameter ranging from 14.5 to 24.5  $\mu\text{m}$  and the average diameter is 21  $\mu\text{m}$  (Figure 5.2.1). The weight of a single Kevlar fiber was determined to be  $1.27 \times 10^{-4}$  mg. The expected number of 10 mg/L concentration of MFs about the was  $7.85 \times 10^4$ , which increased to  $7.85 \times 10^5$  at a concentration of 100 mg/L (Table 5.2.1). The cotton fibers were the most frequently found to have diameters ranging from 14 to 20  $\mu\text{m}$ . The average diameter of 18  $\mu\text{m}$  corresponded to the weight of one cotton MFs at  $9.36 \times 10^{-5}$  mg for a length of 250  $\mu\text{m}$  (Figure 5.2.2). At the concentration of 10 mg/L the estimated number of MFs was  $1.07 \times 10^5$  increased to  $1.07 \times 10^6$  to the concentration of 100 mg/L (Table 5.2.1). PAN exhibited the highest frequency of fiber diameter within the range of 16–22  $\mu\text{m}$  and average diameter was 21  $\mu\text{m}$  with the single fiber weight of  $1.02 \times 10^{-4}$  mg (Figure 5.2.3). At the concentration of 10 mg/L the estimated number of MFs was  $9.78 \times 10^4$  and at a concentration of 100 mg/L it was  $9.78 \times 10^5$  (Table 5.2.1). In the case of PES the highest frequency of fiber diameter was observed within the range of 19–23  $\mu\text{m}$  with the single fiber weight of  $1.16 \times 10^{-4}$  mg (Figure 5.2.4). The estimated number of 10 mg/L the concentration of MFs was  $8.60 \times 10^4$  and at the concentration of 100 mg/L it was  $8.60 \times 10^5$  (Table 5.2.1).

## Confirmation of MFs by FTIR

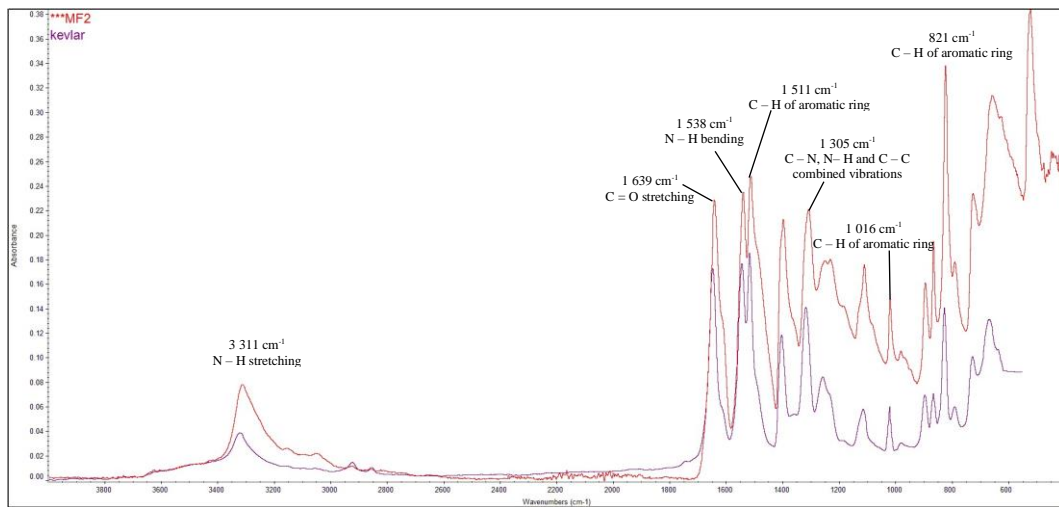


Figure 4.2.5: FTIR spectrum of Kevlar MFs

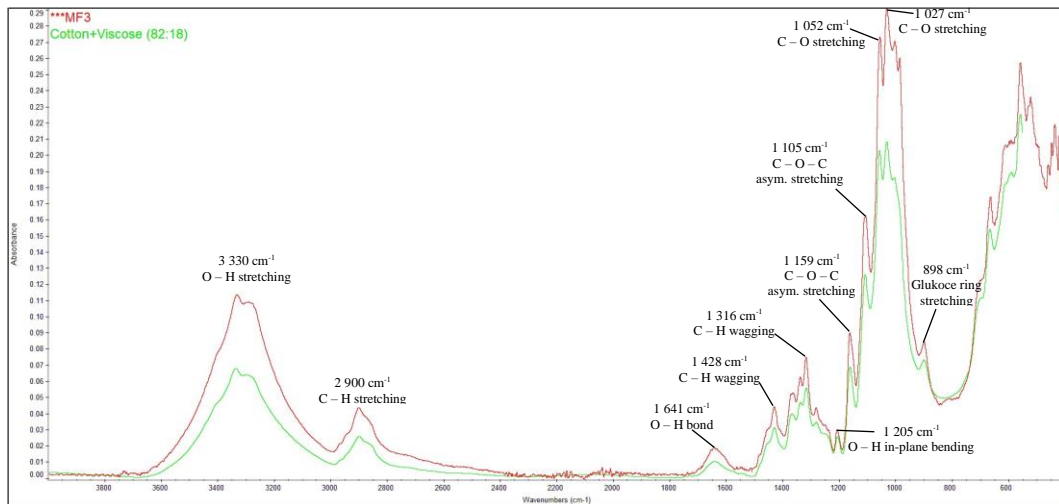


Figure 4.2.6: FTIR spectrum of Cotton MFs

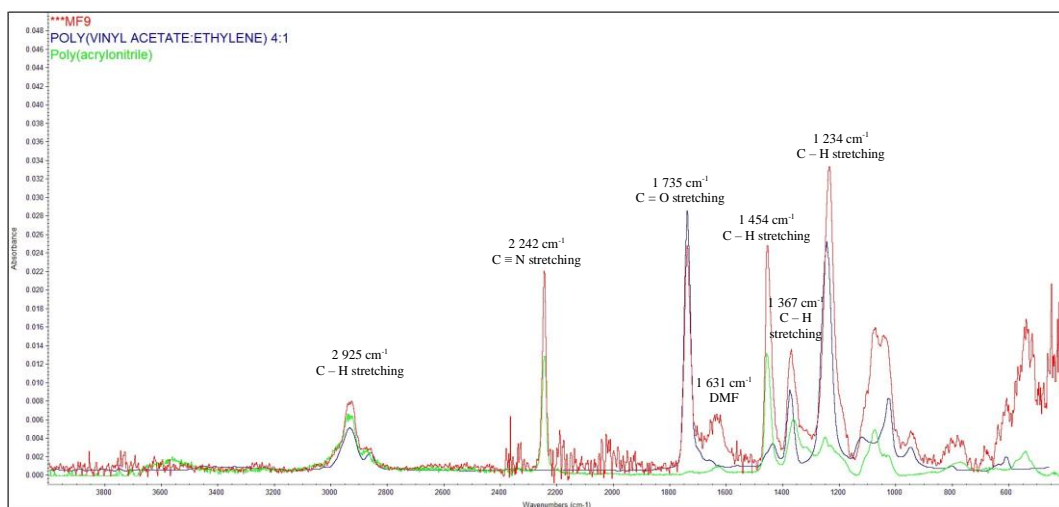


Figure 4.2.7: FTIR spectrum of PAN MFs



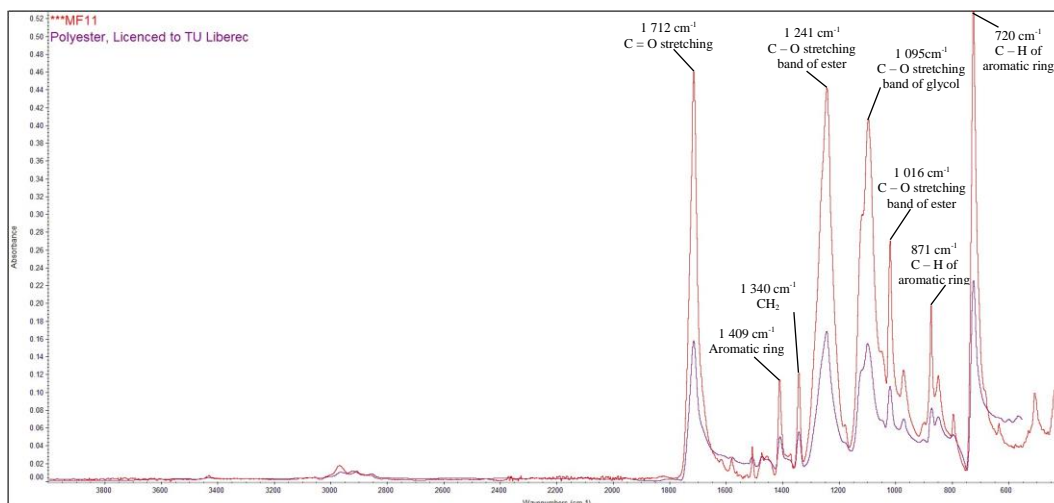


Figure 4.2.8: FTIR spectrum of PES MFs

The spectrum of the kevlar MFs was compared to the known sample (Figure 4.2.5), showing significant peaks. Peaks at  $3311\text{ cm}^{-1}$  represented N-H stretching vibrations while another one at  $1639\text{ cm}^{-1}$  indicated C=O bond stretching in amide group. The double peak at  $1538\text{ cm}^{-1}$  and  $1511\text{ cm}^{-1}$  revealed C-N bond stretching and C-N-H deformation vibrations characteristic of para-aramid. Weak signals at  $1305\text{ cm}^{-1}$  indicated deformation vibrations from N-H and OCN groups in secondary amides, attributed to polyamides (Almarroof et al., 2019; Derombise et al., 2010).

The sample spectrum of cotton MFs was compared to the known sample of cotton and viscose in the 82:18 ratio, both displaying similar peaks (Figure 4.2.6). FTIR analysis of cotton displayed characteristic bands associated with cellulose, primarily found in cotton MFs. The cellulose structure corresponded to peaks at  $3330\text{ cm}^{-1}$ ,  $2900\text{ cm}^{-1}$ ,  $1159\text{ cm}^{-1}$ ,  $1105\text{ cm}^{-1}$ ,  $1027\text{ cm}^{-1}$ ,  $1052\text{ cm}^{-1}$ . The presence of water in cellulose was evidenced by the absorption peak at  $1641\text{ cm}^{-1}$ , corresponding to OH stretching vibrations (Chung et al., 2004; Nam et al., 2015).

The spectrum of the PAN sample was compared to the known samples of polyacrylonitrile (PAN) and poly(vinyl acetate: ethylene) in the 4:1 ratio (Figure 4.2.7). A noticeable difference from pure PAN was observed when compared to polyacrylonitrile. When it was compared to poly(vinyl acetate: ethylene) in a 4:1 ratio, some similar peaks were identified ( $1735\text{ cm}^{-1}$ ). The presence of dimethylformamide (DMF) solvent at  $1631\text{ cm}^{-1}$  was commonly used in PAN MFs production persisted as an impurity in PAN. The bond stretching of C=O at  $1735\text{ cm}^{-1}$ , typical for amides, was thus associated with DMF. These discoveries offered insights

into the molecular composition and structural properties of PAN copolymers facilitating their utilization across various industries (Sülar and Devrim, 2019; Mahltig, 2021).

The spectrum of the PES MFs closely resembled the known polyester, that shared similar characteristics (Figure 4.2.8). These findings offered comprehensive insights into the molecular composition and structural properties of PES. The strong peaks were shown at  $1712\text{ cm}^{-1}$ ,  $1241\text{ cm}^{-1}$ ,  $1095\text{ cm}^{-1}$  and  $720\text{ cm}^{-1}$  corresponded to the C=O stretching vibration, C-O stretching vibrations of ester, C-O stretching vibrations of glycol and aromatic C-H vibrations. At  $1409\text{ cm}^{-1}$ ,  $340\text{ cm}^{-1}$ ,  $10616\text{ cm}^{-1}$  and  $871\text{ cm}^{-1}$  medium peaks were detected for aromatic ring vibration, alkane vibrations, C-O stretching band of ester, and C-H vibrations of aromatic ring (Silva et al., 2012; Sülar and Devrim, 2019).

### **4.3 Growth curve of isolated AS bacteria**

As a bachelor's student, this work was my very first step in the research path. Bacterial growth curves were performed to be familiar with the methods and bacteria. The methodologies were carefully selected to offer the comprehensive understanding of bacterial growth dynamics. OD600 is a method that is normalized based on the chosen blank sample. It represents a rapid and easily deployable technique for gauging variations in bacterial growth. It gives its direct correlation with cell concentration in the sample. CFU was employed as an adjunct method. This approach facilitated the determination of viable bacterial counts per milliliter.

To evaluate the impact of fibers on OD600 measurements, assessments were conducted solely with fibers suspended in AS water. As all utilized fibers possess a greater density than water, they settled on the bottom of the cuvettes. Consequently, the overall sample density approached zero, rendering the influence on measurements negligible.

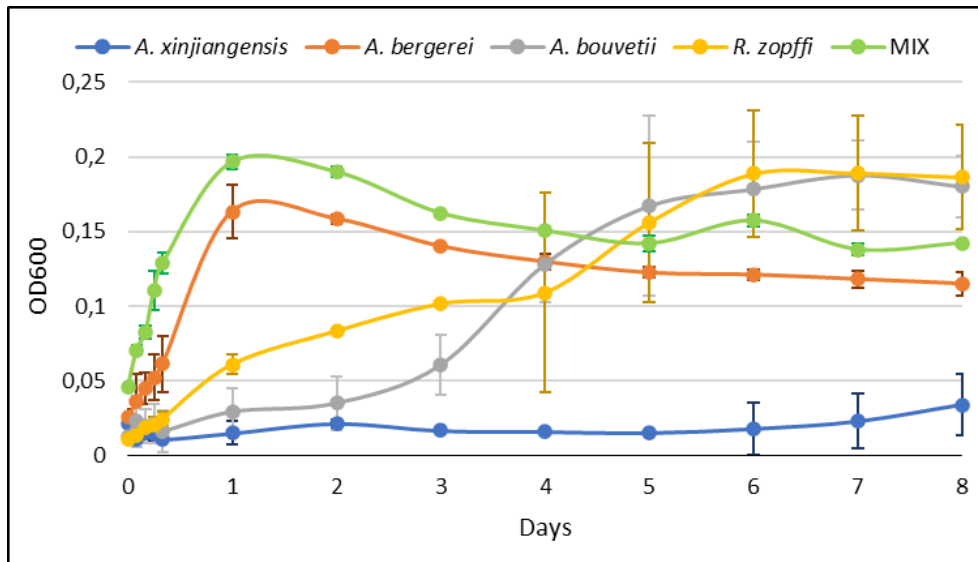


Figure 4.3.1: The cell density (OD600) of each isolated bacterial culture after 8 days

The growth of *A. xinjiangensis* was the slowest compared to *G. bergerei*, *A. bouvetii*, and *R.zopfii*. The exponential phase was not shown in the curve. The exponential phase of *G. bergerei* and the mix were similar after 2 days, while the mix showed higher density compared to *G. bergerei* alone. The growth of *A. bouvetii* and *R. zopfii* was exponential after 5 days and *R.zopfii*'s density was lower compared to Figure 4.3.1.

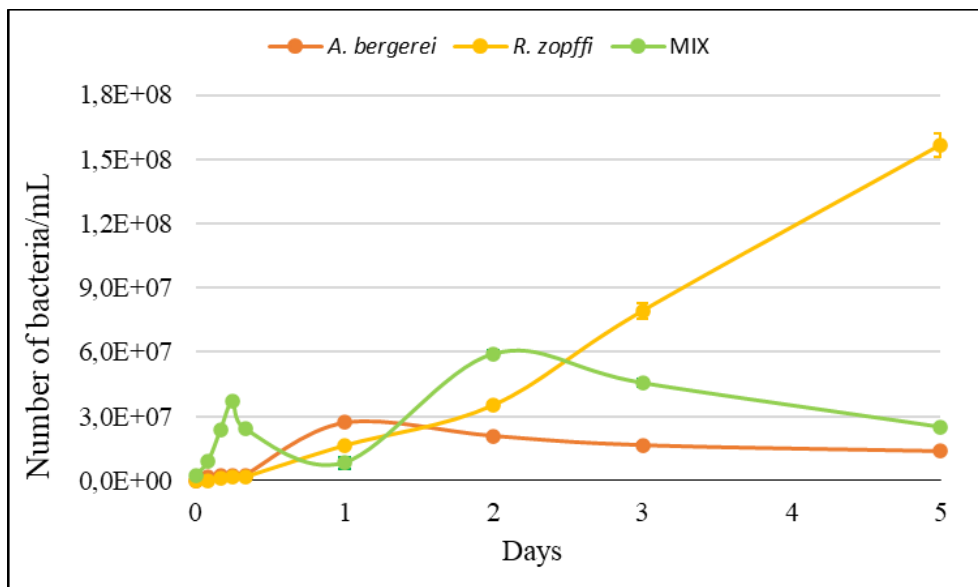


Figure 4.3.2: Determination of the number of viable bacteria per milliliter (CFU/mL): 2 isolated bacterial cultures and MIX after 5 days by CFU

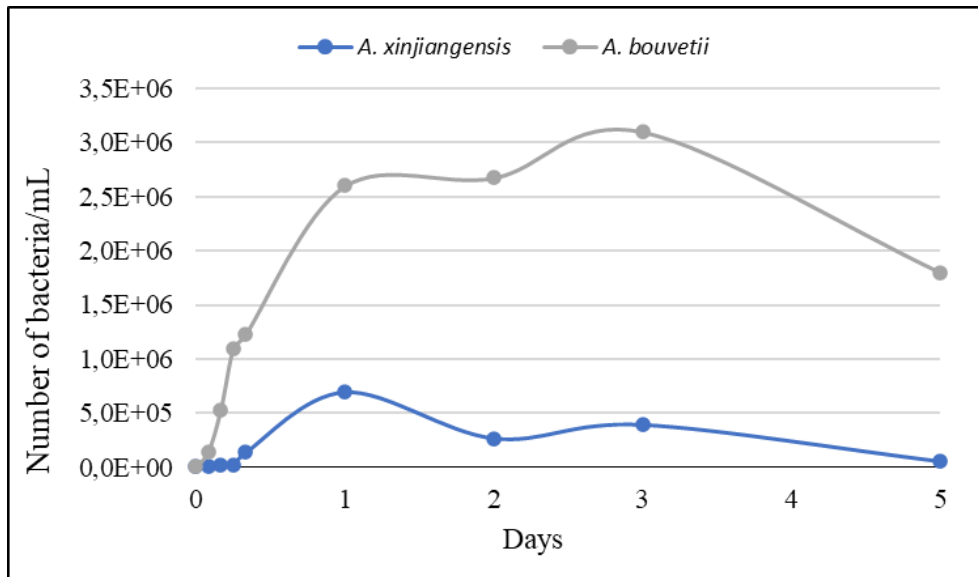


Figure 4.3.3: Determination of the number of viable bacteria per milliliter (CFU/mL): 2 isolated bacterial cultures after 5 days by CFU

*R. zopffi* exhibited the longest duration of growth persisting until day 5 with the highest bacterial content recorded at  $1.6 \times 10^8$  per millilitre (Figure 4.3.2). *G. bergerei* displayed a similar exponential phase after 2 days (Figure 4.3.2). Conversely, *A. xinjiangensis* demonstrated the lowest count during the exponential phase measuring  $7 \times 10^5$  per millilitre its growth curve closely resembled to *G. bergerei* (Figure 4.3.3). However the growth trajectory of *A. bouvetii* remains incompletely documented due to the exclusion of two out of three samples in the two final time sampling points because of erroneous dilution procedures (Figure 4.3.3). In the mixed culture the initial growth occurred within the first 8 hours and it was followed by potential shifts in dominant bacterial species after 24 hours given the presence of four bacterial strains. The exponential phases of the mixed culture exhibited similarity after 3 days (Figure 4.3.3).

#### 4.4 Exposure of isolated AS bacteria to MFs

The primary objective was to examine the impact of textile fibers on bacterial behavior, initially assessing changes in cell density through OD600 measurements. The attachment of bacteria to textile fibers was investigated using the scanning electron microscopy (SEM).

#### 4.4.1 *A. bergerei*

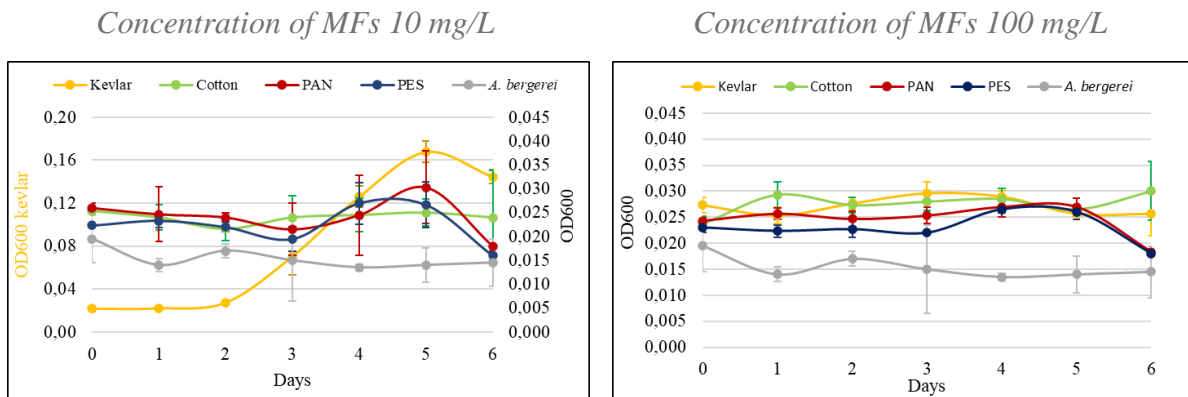


Figure 4.4.1: The density (OD600) of *A. bergerei* exposed to MFs of 10 mg/L and 100 mg/L in AS water medium after 6 days. With 10 mg/L, the left Y-axis is for kevlar, the right Y-axis is for cotton, PAN, PES

The initial focus was on *A. bergerei*, which exhibited a well-defined growth curve during the previous examination at 3.16. However, the growth was not observed during the experiment. The graph depicts five curves. The graph illustrates the density of *A. bergerei* at OD600 when bacteria were exposed to four different MFs at a concentration of 10mg/L. The yellow curve was aligned on the left horizontal axis while the remaining curves correspond to the right horizontal axis. The growth of *A. bergerei* alone remained consistent over time reflecting its behavior when it was exposed to cotton fibers in both concentrations. Different growth was observed when bacteria were exposed to kevlar. When *A. bergerei* were exposed to the 10mg/L concentration of kevlar They resulted in the initial growth since the second day. But the bacteria exposed to the 100 mg/L concentration of kevlar did not have any significant growth. The highest concentration of bacteria was recorded on the third day. The PES sample with *A. bergerei* behaved in the same way in both concentrations of MFs. Any changes in the growth curve were not visible for the first three days. On the fourth day there was the exponential phase and on the sixth day a visible decrease appeared in the concentration of *A. bergerei*. *A. bergerei* with lower concentration of PAN did not grow in the first three days. It can be read that the bacteria slightly decreases until the fourth day when they started to grow. The highest increase in the number of bacteria in the sample was recorded on the fifth day then they decreased on the following days., The curve was not changed in higher concentrations of PAN until the last day when they started to decrease. When *A. bergerei* was exposed to PES and PAN, it behaved quite strangely.

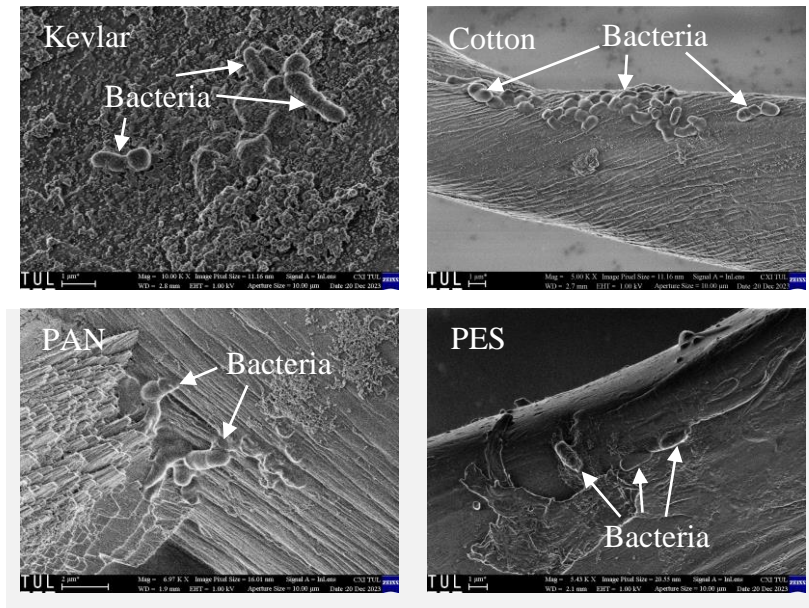


Figure 4.4.2: SEM images. The attachment of *A. bergerei* on MFs

This methodological approach was employed to scrutinize the morphological attributes of bacteria and their interaction with the surface of MFs. The SEM image showed the surface of MFs that were covered with bacteria. The bacteria are observed as round or oval structures with different sizes. Variability in bacterial cell structure can indicate different stages of growth or metabolic activities. Some bacteria were observed as single units, while others aggregate into larger groups and could begin to form biofilms (Figure 4.4.2).

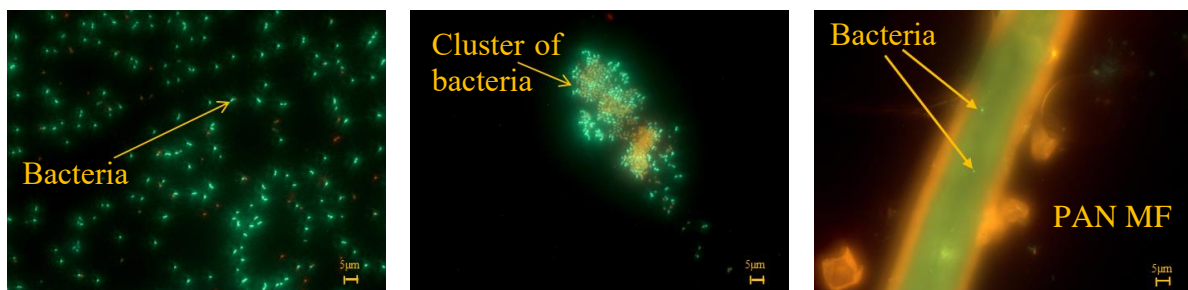


Figure 4.4.3: Images of living bacteria (green fluorescence) and dead bacteria (red fluorescence) obtained by epifluorescence microscope. *A. bergerei* with PAN MFs.

Upon examination with a fluorescence microscope the bacteria were successfully identified. A live bacteria were distinguished by green fluorescence, while a dead bacteria were seen as red fluorescence indicative of membrane damage. The SEM confirmed the presence of bacteria on the surface of the textile fibers. The fluorescence microscopy revealed that the MFs minimally influenced the bacterial growth and environment. Dead cells were observed, their abundance did not differ significantly from the bacterial control sample. The bacterial

mortality was negligible due to interactions with the MFs surface. In containing fibers samples individual bacterial cells and clusters were observed resulting from their adhesion to the surface or interaction between bacteria. In the control sample consisting solely of bacteria some clusters were absent, while some clusters were found in presentation MFs (Figure 4.4.3).

#### 4.4.2 *R. zopffi*

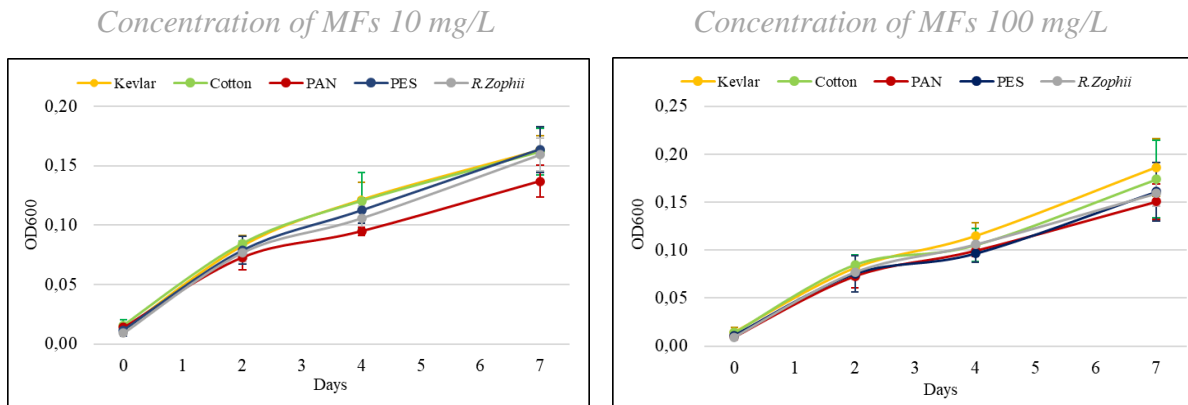


Figure 4.4.4: The density (OD600) of *R. zopffi* exposed to MFs of 10mg/L and 100mg/L in AS water medium after 7 days.

According to the graph (Figure 4.4.4) the population of *R. zopffi* exhibited growth throughout the entire measurement period. The growing trend of the bacterium matched with the growth curve expectation from the experiment in Figure 4.3.2. *R. zopffi* demonstrated similar behavior after five days of incubation. The results from the graphs indicated that the presence of MFs did not have any significant effect on this bacteria growth. By the second day curves of both concentrations of MFs with the bacteria and pure *R. zopffi* were identical. The lowest growth was observed in the samples exposed to PAN at lower and higher MF concentrations. *R. zopffi* in the environment with PES behaved similarly to the control samples of the bacteria in both concentrations. Samples with cotton and kevlar MFs in the concentration of 10 mg/L exhibited growth similar to that of the control samples of the bacteria. These MFs at a concentration of 100 mg/L demonstrated the slightly higher increase in bacterial concentration after four incubation days.

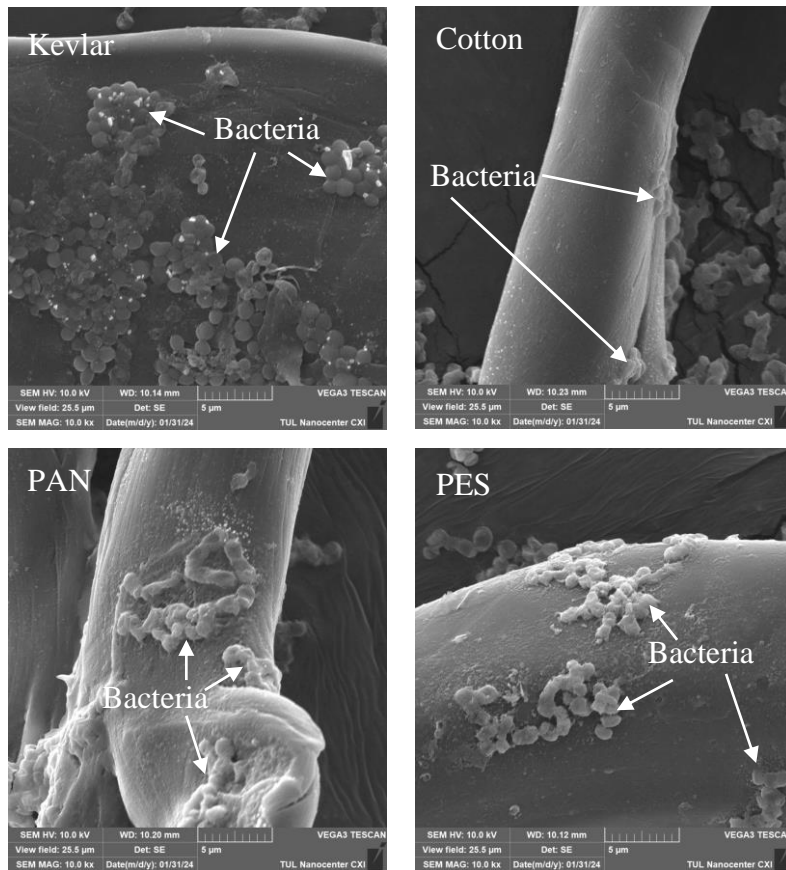


Figure 4.4.5: SEM images. The attachment of *R.zopfii* on MFs

Despite the minimal impact of fibers on *R. zopfii* growth their interaction was visible in SEM images (Figure 4.4.5). *R. zopfii* appeared as spherical structures ranging from 1 to 2 μm. The bacteria were observed in various forms including individual units, aggregates and biofilms. These observations suggested that even with the minimal MFs influence on bacterial growth interaction between bacteria and fiber surface could occur.

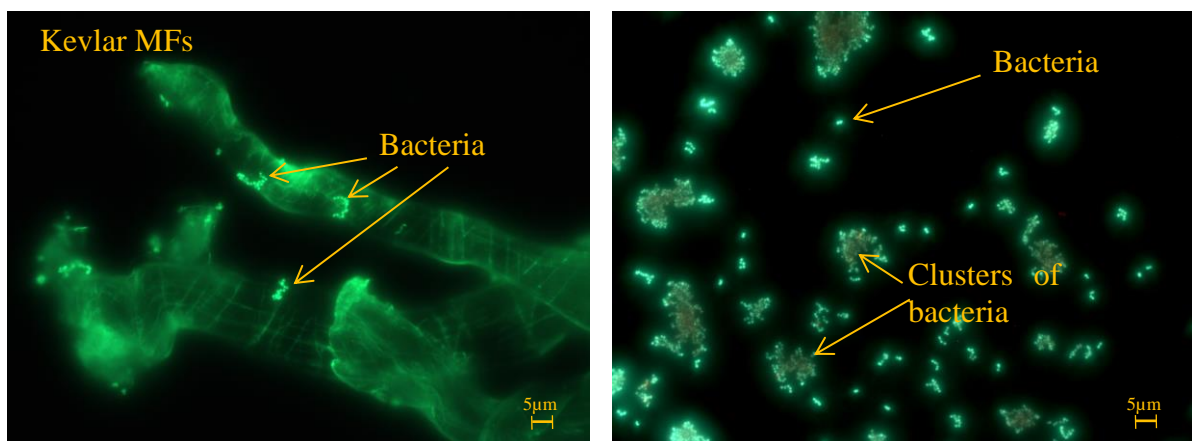


Figure 4.4.6: Images of living bacteria (green fluorescence) and dead bacteria (red fluorescence) obtained by epifluorescence microscope. *R. zopfii* with Kevlar MFs



Overall characterization was supplemented by fluorescence microscopy (Figure 4.4.6). The live and dead bacteria were examined. The interaction between *R. zopfii* and MFs was not well observed. The live bacteria were found up through the measurement period. The number of dead bacteria did not differ significantly compared to the control samples. Both individual and aggregated bacteria were found in all samples.

### 4.4.3 *A. bouvetii*

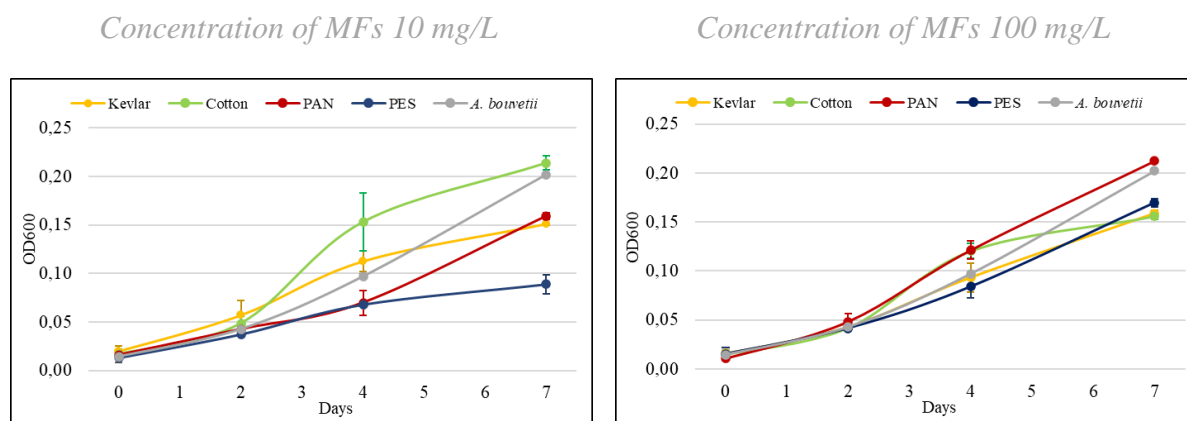


Figure 4.4.7: The density (OD600) of *A. bouvetii* exposed to MFs of 10mg/L and 100mg/L in AS water medium after 7 days.

The growth dynamics curve of *A. bouvetii* aligned closely with the curve depicted in Figure 4.4.7. No significant deviations or mutual differences were observed among the individual samples through the monitoring period. The growth trajectories of *A. bouvetii* exhibited similarity to the second day, when they began to diverge. In the graph illustrating MFs with a concentration of 10 mg/L the sample containing cotton exhibited the highest concentration of bacteria after the second day. The PES sample did not exhibit any increase after the fourth day. The growth of *A. bouvetii* in the presence of kevlar was comparable to the pure bacterial growth till the second day and growth was not observed after the fourth day. The growth in the presence of PAN displayed a linear trend. The concentration of *A. bouvetii* with PAN was comparable to the PES sample on the fourth day and by the fifth day it was similar to the bacterial concentration of the kevlar sample. The growth of the control sample with only bacteria was the nearest to the cotton samples on the last day of observation.

In the graph with MFs 100 mg/L the growth curves were more similar. After the second day the curve of the 10mg/L of PAN sample differed from the higher PAN concentration. The cotton sample exhibited lower bacterial concentrations after the second day and samples exhibited a similar curve trend across different fiber concentrations. The growth curve of *A.*

*bouvetii* in the environments with PES or kevlar was comparable to pure bacterial growth after the second day. The concentrations of both samples reached level similar to that of the cotton sample on the seventh day.

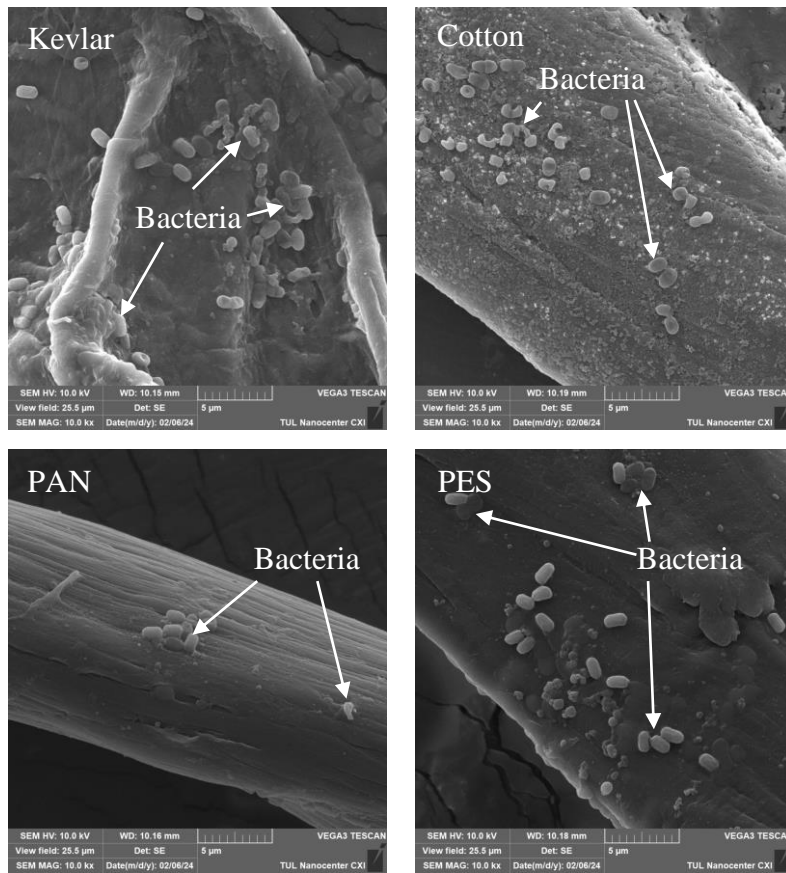


Figure 4.4.8: SEM images. The attachment of *A. bouvetii* on MFs

Figure 4.4.8 presented the results of observations on the attachment of *A. bouvetii* bacteria to various MFs. *A. bouvetii* bacteria were found on these MFs and exhibited oval structures with different sizes. The variability in bacterial cell structure could suggest different stages of growing or metabolic activities. While the majority of visible bacteria appeared on the fibers as individual units, there was also evidence of the aggregation into larger groups.

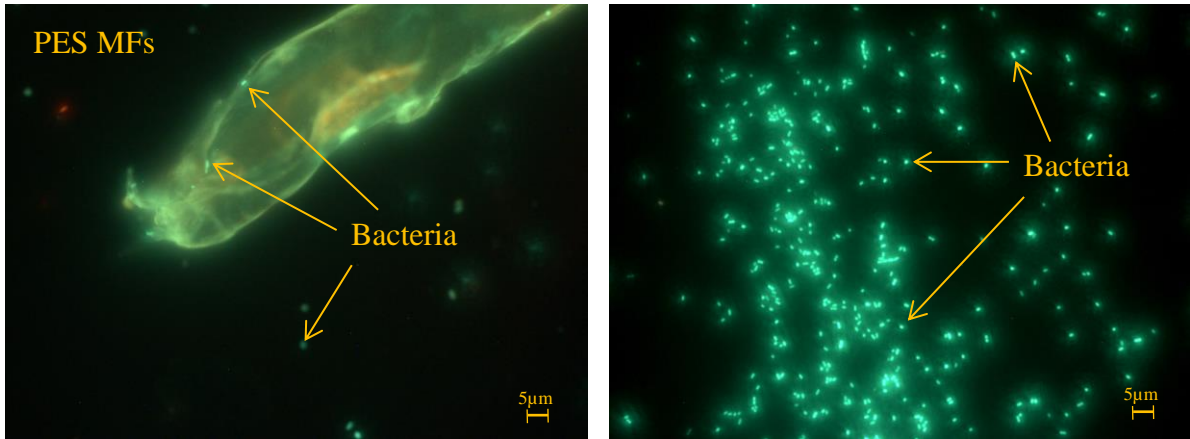


Figure 4.4.9: Images of living bacteria (green fluorescence) and dead bacteria (red fluorescence) obtained by epifluorescence microscope. *A. bouvetii* with PES MFs.

*A. bouvetii* bacteria were examined using the fluorescence microscope (Figure 4.4.9). The number of a live bacteria emitting green fluorescence gradually increased during the measurement period. Dead bacteria did not show any significant increase during the observation period.

#### 4.4.4 *A. xinjiangensis*

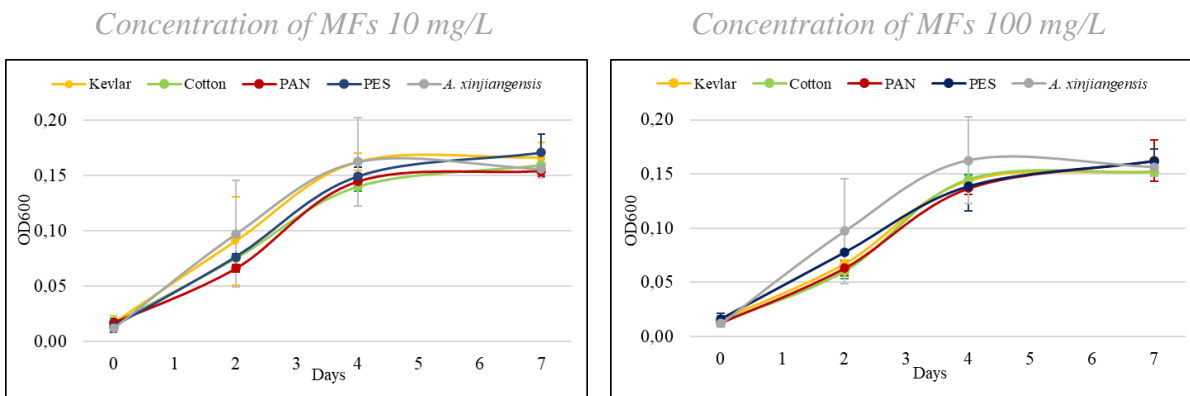


Figure 4.4.10: The density (OD600) of *A. xinjiangensis* exposed to MFs of 10mg/L and 100mg/L in AS water medium after 7 days.

, it was found that graphs representing concentrations of 10 m/L and 100 mg/L exhibited minimal differences in the analysis of the influence of MFs concentrations on the growth of *A. xinjiangensis* bacteria (Figure 4.4.10). This result suggested that in these concentrations any significant effect on bacterial growth was not observed. Growth curves for these concentrations indicate lower values than the pure *A. xinjiangensis* bacteria. The more interesting result was observed in the 10 mg/L concentration of kevlar og sample, which deviated from the other samples. This sample demonstrates a growth dynamic similar to that of the pure bacteria. The stationary growth phase was discovered in all samples around the fourth day

of the incubation period. This temporal point indicated the attainment of the maximum growth point, where the bacterial population was stabilizes in the medium.

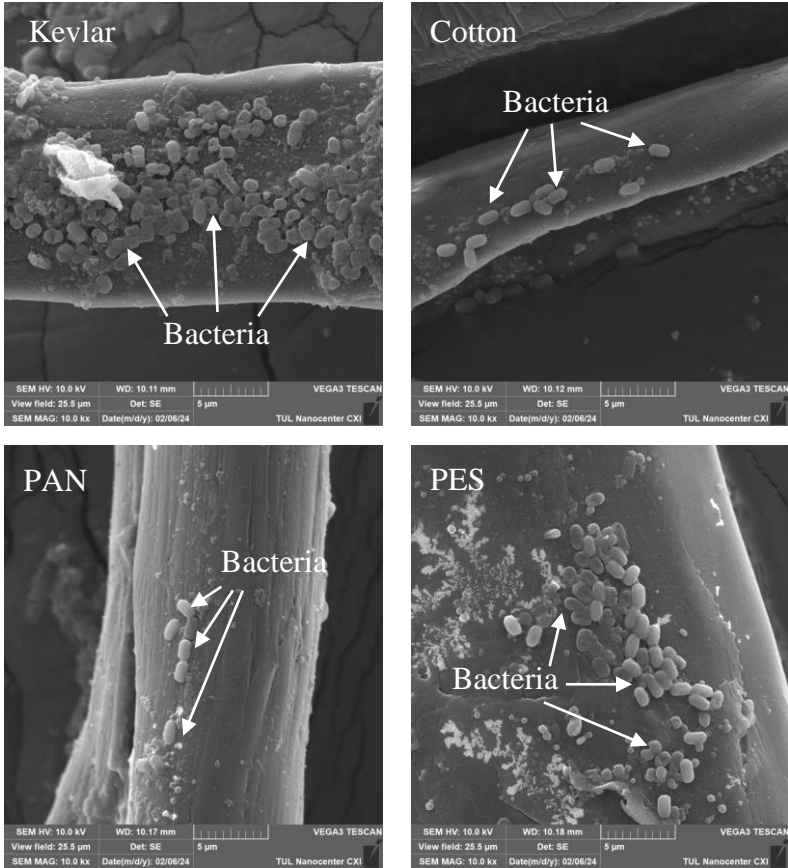


Figure 4.4.11: SEM images. The attachment of *A. xinjiangensis* on MFs

The textile MFs were covered with the bacterium *A. xinjiangensis*. The morphology of these bacteria were oval. The different variability was identified in the structure of bacterial cells. This phenomenon resulted from various growth stages or metabolic activities. The bacteria were mainly found individually, but some signs of bacterial aggregates, also known as clusters or clumps, were observed. Microscopic imaging using SEM exhibited significant similarity with images obtained during the study of the bacterium *A. bouvetii*.

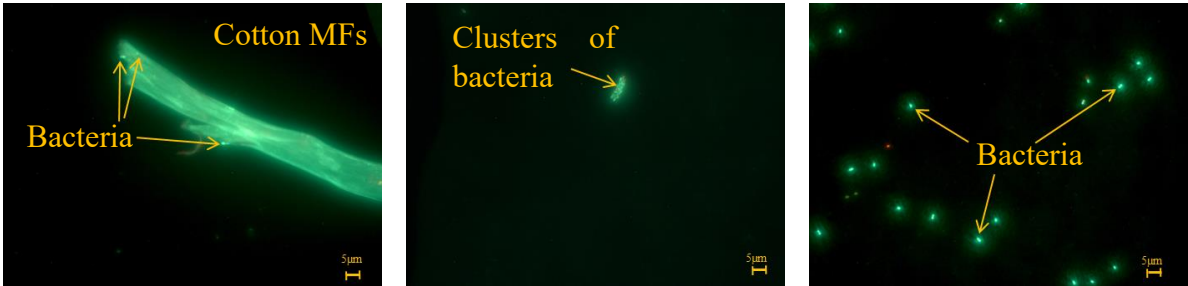


Figure 4.4.12: Images of living bacteria (green fluorescence) and dead bacteria (red fluorescence) obtained by epifluorescence microscope. *A. xinjiangensis* with cotton MFs

This similarity was further confirmed during the subsequent examination of live and dead bacteria using fluorescence microscopy. There were noted comparable trends of observing phenomena in *A. bouvetii* and *A. xinjiangensis*, where the number of live bacteria increased while dead bacteria were not in alarming quantities.

## 4.5 Exposure of AS bacterial community to MFs

### 4.5.1 Extracted DNA concentration

The DNA concentration of the control samples day 0 were compared to the control samples day 8. The samples taken from the control samples day 0 (AS T0, T1, T2, T3) were not constant. The concentration had range from 50 ng/ $\mu$ L to 124 ng/ $\mu$ L. The average value of the samples was determined to 95 ng/ $\mu$ L (Table 4.5.1). These samples were compared with the control samples after 8 days (AS\_a,b,c). The total DNA concentration of control samples day 8 was determined to 62.4 ng/ $\mu$ L. The samples did not reach as high concentrations as control samples day 0. Two filtrations were performed for samples collected after the day 8. The first filtration was done through a 20  $\mu$ m filter (AT) to detect bacteria attached to the MFs. But the bacteria formed a biofilm and also as it was AS water that was not filtered just allowed the sludge to settle. There could be residual sludge where the bacteria could be presented. The higher concentration of DNA was isolated from the 20  $\mu$ m filter. The second 0.2  $\mu$ m filter (FL) captured the free-living bacteria (Table 4.5.1).

The concentration of DNA in Kevlar - AS – FL was 2 to 3 times (15.33 ng/ $\mu$ L) higher than the control sample AS – FL (5.10 ng/ $\mu$ L). On the other hand the average DNA concentration value on filter 20  $\mu$ m was 2 times lower (25.40 ng/ $\mu$ L) than the control sample AS – AT (57.30 ng/ $\mu$ L). The total average of DNA concentration in the samples with Kevlar MFs (Kevlar - AS = 40.73 ng/ $\mu$ L ) was less than 35%. The DNA concentration in the Cotton - AS – FL was 3.5 times (18.10 ng/ $\mu$ L) higher than in the control AS – FL (5.10 ng/ $\mu$ L) and in one sample of the DNA concentration triplet was 5.5 times higher (28.90 ng/ $\mu$ L). The average DNA concentration (44.80 ng/ $\mu$ L) on filter 20  $\mu$ m was 21% less compared to AS – AT (57.30 ng/ $\mu$ L). The DNA concentration of the PAN - AS – FL sample (18.07 ng/ $\mu$ L) was comparable to the Cotton - AS – FL sample (18,10 ng/ $\mu$ L). The DNA concentration (36.23 ng/ $\mu$ L) in the PAN - AS – AT sample had a lower value than the Cotton - AS - AT sample (44.80 ng/ $\mu$ L) and the difference of the control AS – AT sample was 36% less

(57.30 ng/ $\mu$ L). The total concentration of the PAN MFs sample (54.30 ng/ $\mu$ L) was comparable to the PES MFs sample (53.47 ng/ $\mu$ L) and was 13% lower than the control AS sample (62.40 ng/ $\mu$ L). The DNA concentration of PES - AS - FL (15.67 ng/ $\mu$ L) was comparable to the Kevlar - AS - FL (15.33 ng/ $\mu$ L) sample and the PAN - AS - AT (36.23 ng/ $\mu$ L) was similar with the PES - AS - AT (37.80 ng/ $\mu$ L) sample.

Table 4.5.1: DNA concentration of control samples day 0, day 8; samples with MFs after 8 days measured by Qubit fluorometer. AT: bacteria attached on MFs, FL: free-living bacteria

	Sample name	Filter (µm)	DNA concentration (ng/uL)	Average DNA concentration (ng/uL)	Total DNA concentration (ng/uL)
Samples with kevlar MFs after 8 days	Kevlar - AS - FL_a	0.2	17.6	15.33 ± 3.18	40.73 ± 8.39
	Kevlar - AS - FL_b	0.2	11.7		
	Kevlar - AS - FL_c	0.2	16.7		
Samples with kevlar MFs after 8 days	Kevlar - AS - AT_a	20	25.8	25.40 ± 5.21	
	Kevlar - AS - AT_b	20	20		
	Kevlar - AS - AT_c	20	30.4		
Samples with cotton MFs after 8 days	Cotton - AS - FL_a	0.2	10.7	18.10 ± 9.56	62.90 ± 14.42
	Cotton - AS - FL_b	0.2	28.9		
	Cotton - AS - FL_c	0.2	14.7		
Samples with cotton MFs after 8 days	Cotton - AS - AT_a	20	44.9	44.80 ± 4.85	
	Cotton - AS - AT_b	20	49.6		
	Cotton - AS - AT_c	20	39.9		
Samples with PAN MFs after 8 days	PAN - AS - FL_a	0.2	23.7	18.07 ± 4.99	54.30 ± 15.84
	PAN - AS - FL_b	0.2	14.2		
	PAN - AS - FL_c	0.2	16.3		
Samples with PAN MFs after 8 days	PAN - AS - AT_a	20	45.5	36.23 ± 10.85	
	PAN - AS - AT_b	20	24.3		
	PAN - AS - AT_c	20	38.9		
Samples with PES MFs after 8 days	PES - AS - FL_a	0.2	20.7	15.67 ± 4.37	53.47 ± 14.42
	PES - AS - FL_b	0.2	12.9		
	PES - AS - FL_c	0.2	13.4		
Samples with PES MFs after 8 days	PES - AS - AT_a	20	33.5	37.80 ± 9.97	
	PES - AS - AT_b	20	49.2		
	PES - AS - AT_c	20	30.7		
Control samples day 8	AS - FL_a	0.2	6.01	5.10 ± 1.00	62.40 ± 21.65
	AS - FL_b	0.2	4.03		
	AS - FL_c	0.2	5.26		
Control samples day 8	AS - AT_a	20	37.5	57.30 ± 20.65	
	AS - AT_b	20	78.7		
	AS - AT_c	20	55.7		
Control samples day 0	AS T0	0.2	95.53	-	95.16 ± 32.07
	AS T1	0.2	49.79		
	AS T2	0.2	124.00		
	AS T3	0.2	111.34		

## 4.5.2 Next-generation sequencing of 16S rRNA

### Quality of sequencing data

Depth of coverage was used to ensure that the data were reliable and appropriate for the analysis. The distribution of species were depended on the sample size. Each size was defined as the number of individuals or species recorded in a given sample. The data were created in a graph, where the X-axis represented sample size (sample depth) and the Y-axis the number of species (biodiversity). The diversity at a certain point was fully captured and curves was consistent. When the depth of coverage was too low, it could lead to insufficient sensitivity and reliability of the results, while too high the depth of coverage could impose unnecessary cost and computational burden. It was chosen PAN - AS – AT\_c sample with the least amount of sequences for data interpretation (Figure 4.5.1) (Puón-Peláez et al., 2022).

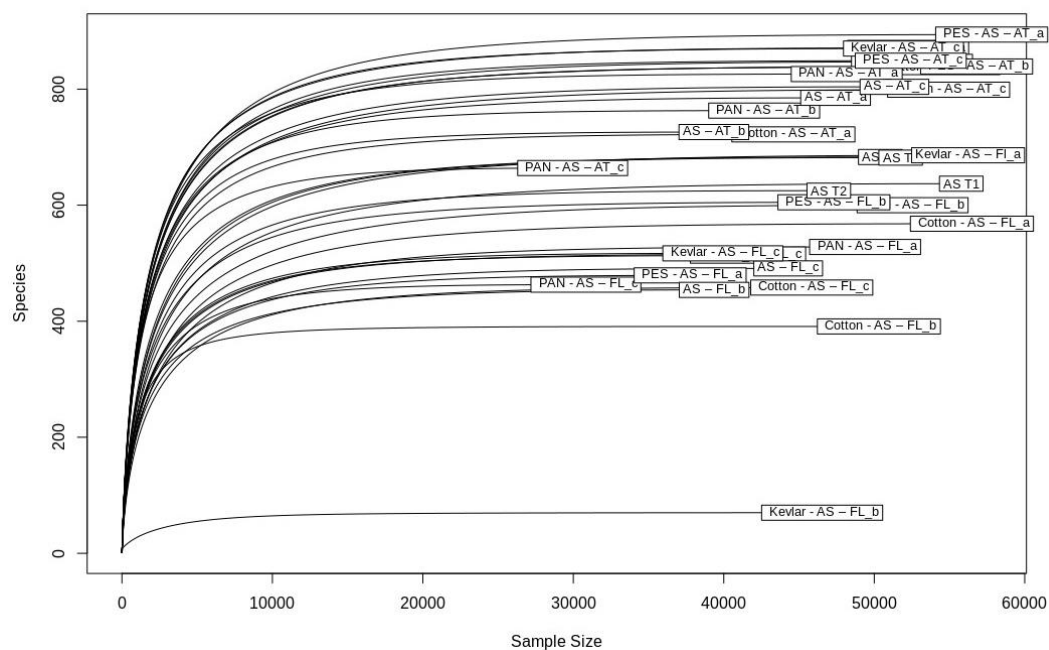


Figure 4.5.1: Rarecurves at amplicon sequence variants (ASV) level

Microbial  $\alpha$ -diversity examined the richness quantified by the number of ASVs (Amplicon Sequence Variant) across a range of samples. Certain points revealed consistent  $\alpha$ -diversity values:

Samples labeled FL (0.2  $\mu\text{m}$  filters) were lower (approximately 500) than the AT bacteria (20  $\mu\text{m}$  filters) with the same MFs (in color boxes, more than 750). AT samples filtered through



20  $\mu\text{m}$  filters (color boxes, Figure 4.5.2) showed greater diversity than the control samples (AS – AT\_a, b, c) and those filtered through 0.2  $\mu\text{m}$  filters (FL). This samples Cotton - AS – FL\_c, AS – FL\_b, PAN - AS – FL\_c, and PES - AS – FL\_a shared the lowest diversity. The diversity value of Cotton - AS – AT\_a corresponded to the value of the control sample AS – AT\_b. Another sample involving cotton, specifically Cotton - AS – AT\_c, exhibited comparable values to control samples AS – AT\_a and AS – AT\_c. Furthermore, samples demonstrating approximately the equivalent  $\alpha$ -diversity included PAN - AS – AT\_a, Cotton - AS – AT\_b, PES - AS – AT\_b, Kevlar - AS – FL\_b, and PES - AS – AT\_c. Finally, the samples with the highest common values were Kevlar - AS – FL\_a, Kevlar - AS – FL\_c, and PES - AS – AT\_a (Figure 4.5.2). There was not any trend for the samples filtered through 0.2  $\mu\text{m}$  filters (FL). Their alpha diversity roughly mirrored the control samples day 8 (AS – FL\_a, b, c) (Figure 4.5.2).

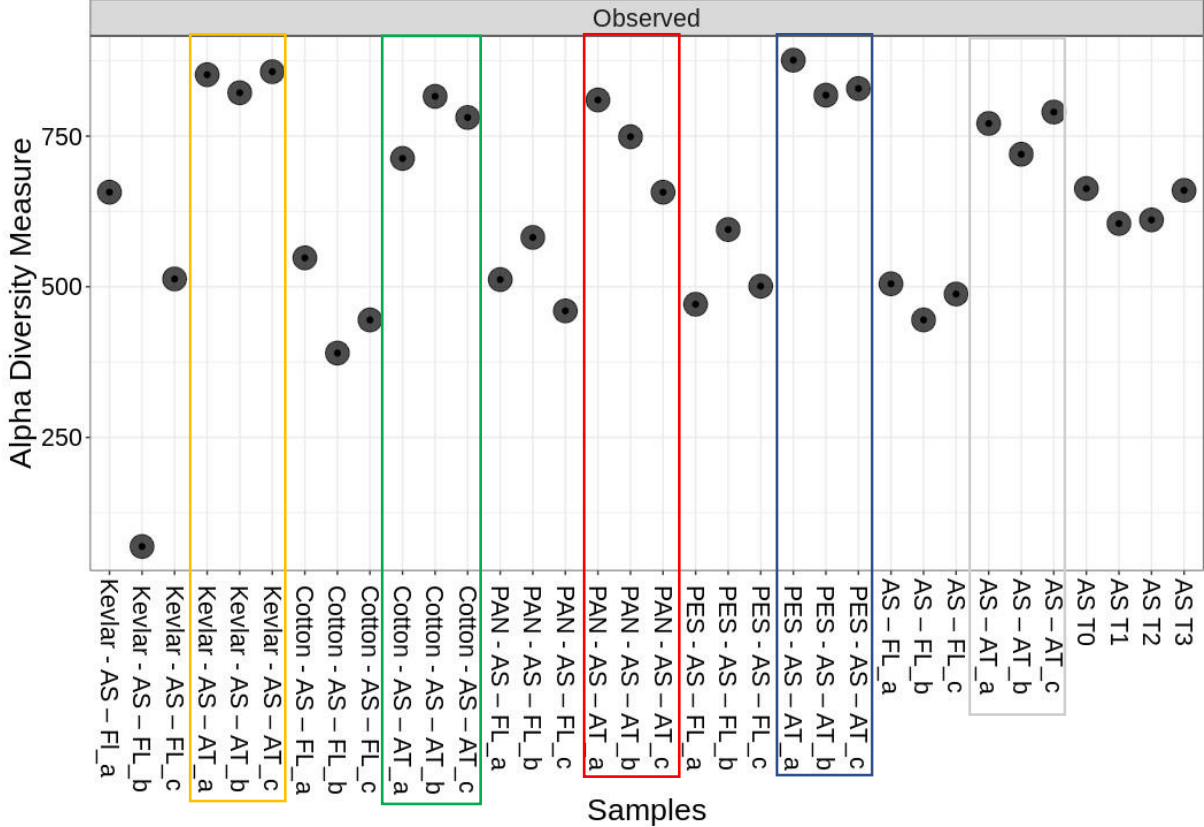


Figure 4.5.2: Alpha diversity of control samples day 0, day 8 and samples with MFs after 8 days at ASV level

### **Relation of samples in genus level**

PCoA (Principal Coordinates Analysis) was performed on microbiome data at the taxonomic levels of ASV and genus using the Bray-Curtis dissimilarity score matrix. The X-axis and Y-axis denoted two principal coordinate axes and the percentage value interprets the difference in sample compositions on these axes. The closer two points on the graph were, the more similar their bacterial genus or ASV composition were. PCoA analysis revealed significant differences in the structure and composition of bacterial communities between the different sample types (Dimkić et al., 2023).

The bacterial taxa were analyzed at the genus level for greater precision (Figure 4.5.4). The graph showed clusters of samples which were similar to their microbial compositions. Samples with increasing distance between them could indicate greater diversity or distinct bacterial communities. One cluster consists of control samples day 0 (grey ring) were different from all other samples. The similarity between the control samples day 8 and the samples with MFs (Kevlar, PAN and PES) was recorded on filters with the same pore size (20  $\mu\text{m}$ , 0.2  $\mu\text{m}$ ) but they showed differences in microbial composition between the two filters. Samples with AT filter (20  $\mu\text{m}$  filters) were marked in the orange ring and FL (0.2  $\mu\text{m}$ ) were marked in the violet ring. A difference was also observed between the bacterial community with cotton (in green) and the other samples with MFs (Kevlar, PAN, and PES) (Figure 4.5.4). The samples with cotton were varied depending on the filters (20  $\mu\text{m}$  dark green, 0.2  $\mu\text{m}$  light green) (Figure 4.5.4).

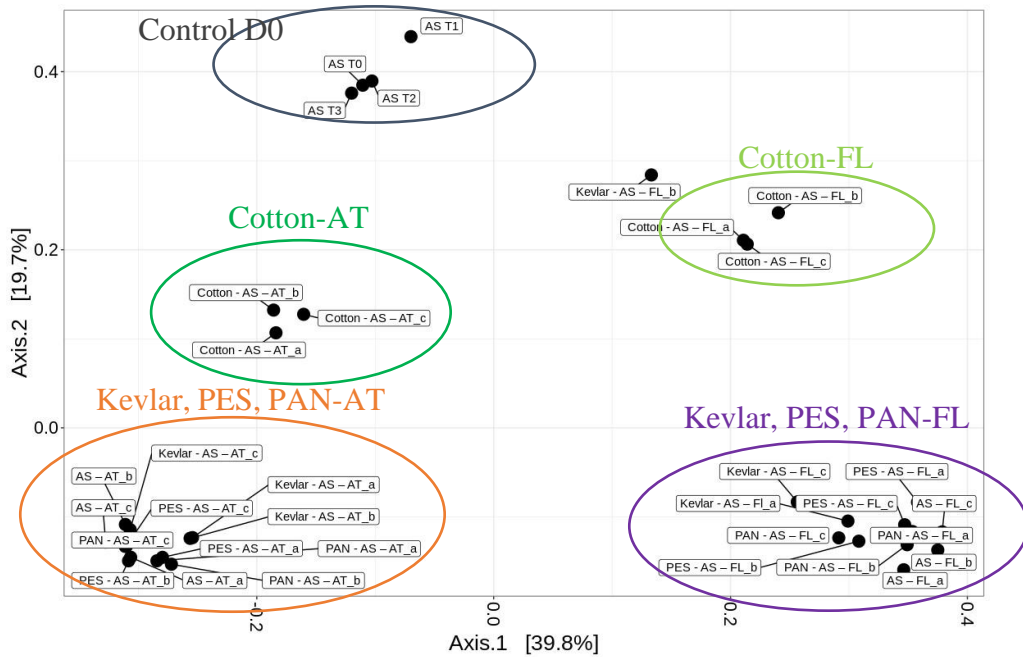


Figure 4.5.3: Principal coordinate analysis (PCoA) of Bray-Curtis distances between samples at genus level

### Taxonomy of bacterial community

The mean taxonomy was examined at the genus level at abundances greater than 0.01. In control samples day 0 (AS T0, T1, T2, T3) the most abundant taxonomic groups were *Flavobacterium*, the family *Comamonadaceae*, and *Pseudarcobacter*. Family *Comamonadaceae* had consistent abundance in control samples day 8 and in samples with Kevlar, PAN and PES MFs after 8 days. While *Flavobacterium* showed a decrease in control samples day 8 and samples with Kevlar, PAN and PES MFs after 8 days, where abundance did not change significantly. The *Pseudarcobacter* genus was attached (AT) and also free-living (FL) were found only in samples containing cotton in trace amounts. Other genera were also represented a lesser extent in control samples day 0, such as env. *OPS 17*, *Methylothera*, *Pseudomonas*, *Zoogloea*, which abundance remained stable after 8 days. The free-living *Pseudomonas* showed less abundance when they were exposed to cotton (Cotton - AS - FL). *Zoogloea* was found in the AT the control samples day 8 and in the AT samples with MFs.

*Dokdonella* was presented in low abundance in the control samples day 0, but its abundance increased in the control samples day 8 and in samples with Kevlar, PAN and PES MFs after 8 days. *Dokdonella* and *Nitrospira* were present in the control samples day 0 with low abundance. In AT the control samples day 8 and AT the samples with MF kevlar, PAN and PES the abundance was much higher than in the control samples day 0. There was smaller representations in AT samples with cotton. FL control samples day 8 and samples with kevlar, PAN

and PES MFs after 8 days were similar to the control samples day 0 except samples with cotton, where they were not found.

The family *Rhodocyclaceae* had the same abundance in the control samples day 0 and the AT control samples day 8 as well as in the samples AT and FL with Kevlar, PAN and PES MFs, but there was an increase in abundance in the samples At and FL with cotton. There was the family *Enterobacteriaceae* in all samples, but any particular trend was not observed. The families *Saprospiraceae*, *Haliangium* and *OLB12* were in the control samples day 0 and were found in the AT samples after 8 days with the same abundance. *Sulfuritalea* was equally represented in the samples and was found in both the sludge (AT) and free-living (FL). *Sulfuritalea* was slightly higher in the AT samples with kevlar and cotton than in other samples. The *Rhodofera* genus showed reduced abundance in other samples compared to control samples day 0.

Control samples day 8 contained *Limnobacter*, NS 11-12\_marine group, *Pedobacter*, *Polynucleobacter*, *Perlucidibace*, *Sediminibacterium* and *Shingorhabdus* unlike control samples day 0. The genus *Limnobacter* was mainly in the free-living form (FL) in the control samples day 8 and the samples with all MFs with its highest abundance in the control samples day 8 and the lowest in the cotton samples. *Limnobacter* was found in the AT control samples day 8, as well as in the samples with Kevlar, PES and PAN, it was not detected in cotton.

The NS 11 - 12\_marine group was mainly present in the FL samples except the FL cotton samples, where abundance decreased. *Polynucleobacter*, *Perlucidibace*, *Sediminibacterium* and *Shingorhabdus* were found in the free-living form. *Sediminibacter* attached in the samples AT on kevlar (yellow box), cotton (green box) and PAN (red box) unlike the control sample (grey box), where it was not on the filter 20 µm. *Perlucidibaca* was attached on PES (blue box) and also in one sample on PAN (red box).

From these results it can be concluded that MFs made of Kevlar, PAN and PES did not have any significant effect on the bacteria community and their abundance was comparable to the control samples day 8. The dominant genus were *Escherichia Shigella* and *Pseudomonas* in the sample with Kevlar fibers, Kevlar - AS – FL\_b. The Kevlar - AS – AT\_b sample showed that the bacteria of the sludge or on the MFs were similar to the bacteria found in the other AT samples of the triplicate, but different from the free-living bacteria (FL). MFs made from cotton showed a different bacterial composition than at the synthetic fibres. In the cotton samples

*Magnetospirillum* was the most distinct free-living (FL) bacteria as well as *Pseudarcobacter* and the family *Cellvibrionaceae*, which were mainly in the AT samples (the green box) (Figure 4.5.4).

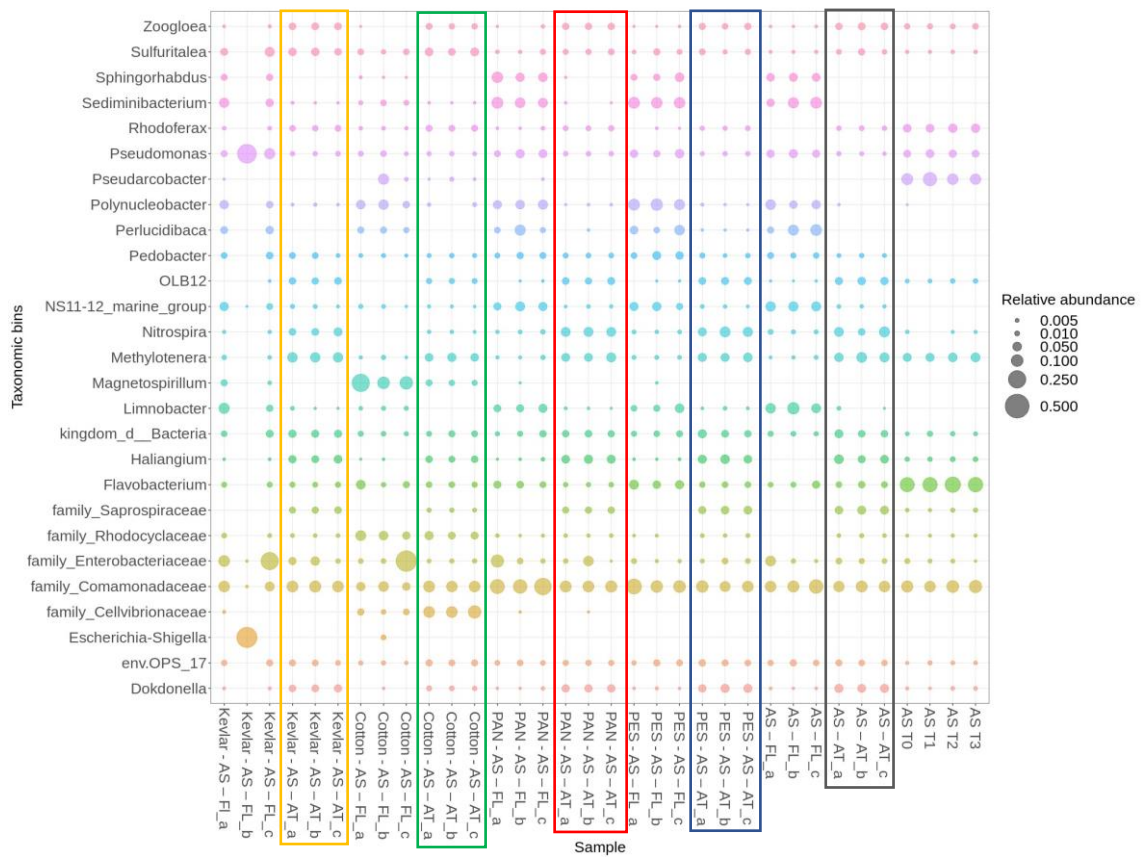


Figure 4.5.4: Taxonomy of bacterial community at genus level

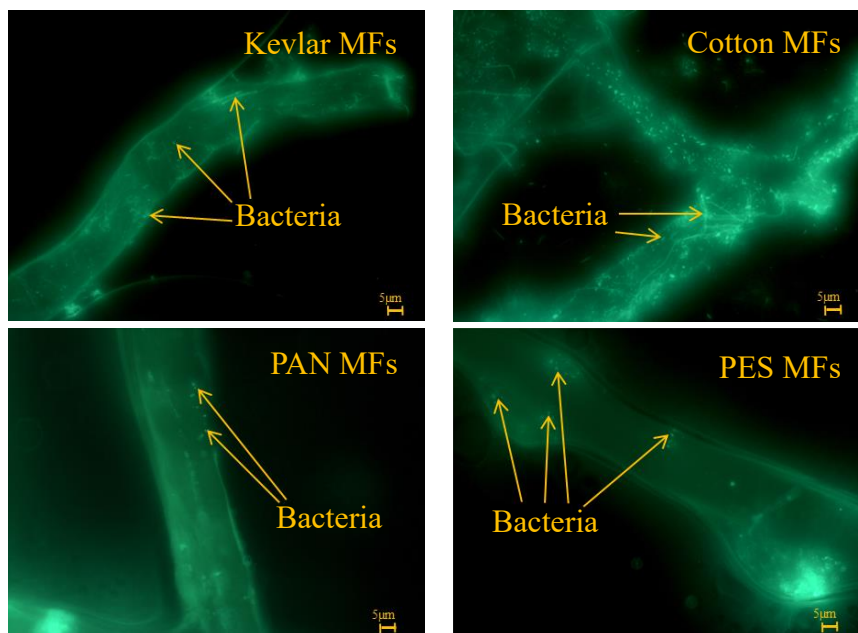
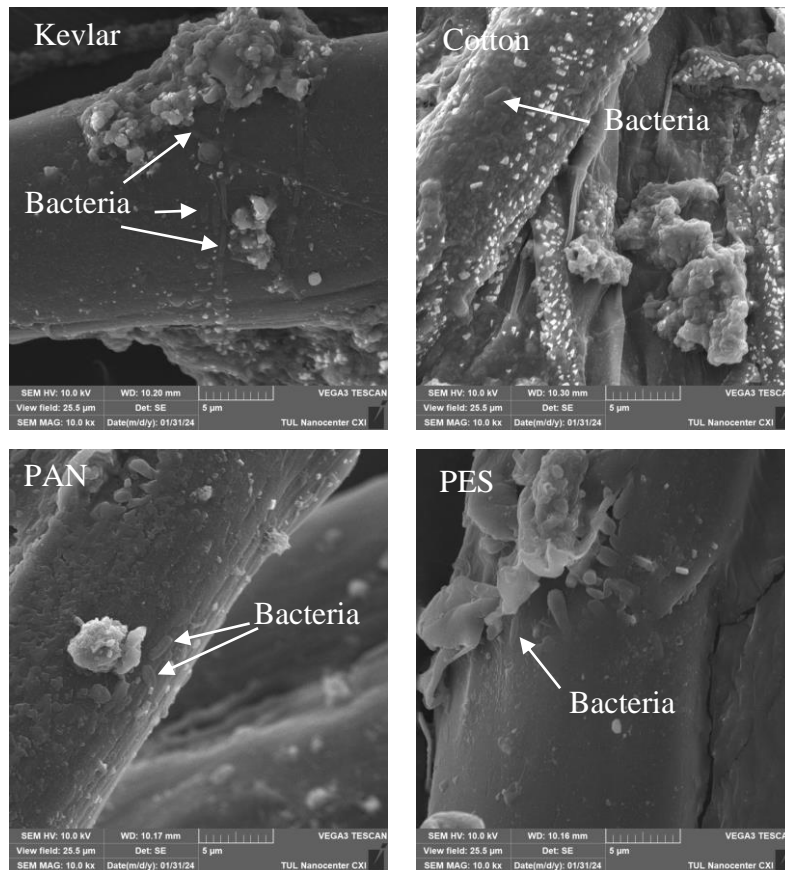


Figure 4.5.5: Images of living bacteria (green fluorescence) obtained by epifluorescence microscope

The bacterial community was observed under the epifluorescence microscope. It was found more abundant attached to cotton MFs against the others (Kevlar, PAN and PES). All samples of microorganisms were in single units or in clusters and could form biofilms (Figure 4.5.5). The detailed observations were made by SEM.



*Figure 4.5.6: SEM images. The attachment of the AS community on MFs*

Bacteria of various shapes and sizes were observed on the surface of the MFs. Some bacteria could appear as single cells, while the others could be observed as clusters or aggregations formed biofilms. The morphology of the bacteria includes round, rod-shaped or coccial cells. AS water substances were also examined of SEM (Figure 4.5.6).

## 5 Conclusion

This study investigated the behavior of microorganisms (1) four isolated bacteria and (2) a bacterial community from AS water collected from the Liberec Wastewater Treatment Plant. It focused on bacteria that were exposed to four types of textile MFs: Milled Kevlar fibers (kevlar), White milled cotton fibers (cotton), Milled acrylic fibers (PAN) and Milled polyester fibers (PES) for 8 days. MFs were used in concentrations of 10 mg/L and 100 mg/L exposed to isolated bacteria, while 100 mg/L exposed to the bacterial community. The growth curves of isolated AS bacteria and the characterization of MFs were studied before performing two experiments.

*G. bergerei* and *A. xinjianenesis* recorded faster growth in comparison to *A. bouvetii* and *R. zopffi*. The diameter of Kevlar, PAN and PES MFs was consistent at 21  $\mu\text{m}$ , while the diameter of cotton MFs was determined to 18  $\mu\text{m}$ . A trend between fiber amount and density was noted for synthetic MFs with denser fibers exhibiting fewer fibers in each sample. This trend was not hold for cotton, despite having the highest density among all fibers, the highest fiber count was observed in the sample with cotton. The fiber structure could be verified through FTIR analysis. All MFs spectra were compared with the spectra of the known samples. MFs kevlar, cotton and PES spectra aligned with the defined polymers. Only PAN differed because of the fibre structure of copolymer poly(acrylonitrile) due to the manufacturing processes employed.

In the first experiment the isolated AS bacteria were exposed to 4 MFs (10 and 100 mg/L) in the sterilized AS water medium. The cell density results showed that optical density (OD) did not have any alarming negative impact of MFs on the four isolated bacteria. A smaller increase was seen at *R. zopffi* in both concentrations of PAN MFs. *A. bouvetii* exhibited various behavior for each MFs concentration making it impossible to discern any trend. The growth curves of *A. xinjianenesis* were lower for all MFs beside the pure control sample of *A. xinjianenesis*. The clustering of bacteria *R. zopffi*, *G. bergerei* and *A. xinjianenesis* was followed during all time. Any significant clusters were not observed for *A. bouvetii*. The adhesion of bacteria to MFs was confirmed through the SEM analysis, where all four bacteria were found attached to MFs. It meant that the bacteria could form biofilms on all MFs.

The second experiment explored 4 MFs (100 mg/L) with the AS bacterial community. The results discovered that alpha diversity had various species in each sample. Only one sample with kevlar MFs showed very little diversity of bacterial species. The  $\alpha$ -diversity values

revealed similar species across individual samples. One sample with Kevlar had the very low diversity of bacterial species. This trend was also evident in the PCoA analysis and in the taxonomic evaluation, where only two dominant species (*Escherichia Shigella* and *Pseudomonas*) were identified. The difference in the structure of the AS community was evident from these two analyses. Synthetic MFs corresponded to the taxonomy of the control sample after 8 days. The samples with cotton exhibited an affinity for different species (particularly *Magnetospirillum*, *Pseudarcobacter*, and the family *Cellvibrionaceae*).

Even though the AS bacterial community was incubated with MFs, It was found that bacteria developed and attached MFs. The attachment could increase when the incubation is prolonged. The cotton as as the natural material showed the higher abundant taxa of both attached and free-living bacteria than the synthesis MFs. The attachment of bacteria on MFs could present coated MFs leading to harmful human risk. For example, when attached bacteria possess antibiotic resistance genes and potentially transfer them and spread the antibiotic resistance.



## References

ALMAROOF, Ahmed, ALI, Ahmed, MANNOCCI, Francesco and DEB, Sanjukta, 2019. Semi-interpenetrating network composites reinforced with Kevlar fibers for dental post fabrication. *Dental Materials Journal*. 30 July 2019. Vol. 38. DOI 10.4012/dmj.2018-040.

BHARDWAJ, Laxmi Kant, RATH, Prangya, YADAV, Poornima and GUPTA, Urvashi, 2024. Microplastic contamination, an emerging threat to the freshwater environment: a systematic review. *Environmental Systems Research*. Online. 28 February 2024. Vol. 13, no. 1, p. 8. DOI 10.1186/s40068-024-00338-7. [Accessed 27 April 2024].

BOLYEN, Evan, RIDEOUT, Jai Ram, DILLON, Matthew R., BOKULICH, Nicholas A., ABNET, Christian C., AL-GHALITH, Gabriel A., ALEXANDER, Harriet, ALM, Eric J., ARUMUGAM, Manimozhiyan, ASNICAR, Francesco, BAI, Yang, BISANZ, Jordan E., BITTINGER, Kyle, BREJNROD, Asker, BRISLAWN, Colin J., BROWN, C. Titus, CALLAHAN, Benjamin J., CARABALLO-RODRÍGUEZ, Andrés Mauricio, CHASE, John, COPE, Emily K., DA SILVA, Ricardo, DIENER, Christian, DORRESTEIN, Pieter C., DOUGLAS, Gavin M., DURALL, Daniel M., DUVALLET, Claire, EDWARDSON, Christian F., ERNST, Madeleine, ESTAKI, Mehrbod, FOUQUIER, Jennifer, GAUGLITZ, Julia M., GIBBONS, Sean M., GIBSON, Deanna L., GONZALEZ, Antonio, GORLICK, Kestrel, GUO, Jiarong, HILLMANN, Benjamin, HOLMES, Susan, HOLSTE, Hannes, HUTTENHOWER, Curtis, HUTTLEY, Gavin A., JANSSEN, Stefan, JARMUSCH, Alan K., JIANG, Lingjing, KAEHLER, Benjamin D., KANG, Kyo Bin, KEEFE, Christopher R., KEIM, Paul, KELLEY, Scott T., KNIGHTS, Dan, KOESTER, Irina, KOSCIOLEK, Tomasz, KREPS, Jorden, LANGILLE, Morgan G. I., LEE, Joslynn, LEY, Ruth, LIU, Yong-Xin, LOFTFIELD, Erikka, LOZUPONE, Catherine, MAHER, Massoud, MAROTZ, Clarisse, MARTIN, Bryan D., MCDONALD, Daniel, MCIVER, Lauren J., MELNIK, Alexey V., METCALF, Jessica L., MORGAN, Sydney C., MORTON, Jamie T., NAIMEY, Ahmad Turan, NAVAS-MOLINA, Jose A., NOTHIAS, Louis Felix, ORCHANIAN, Stephanie B., PEARSON, Talima, PEOPLES, Samuel L., PETRAS, Daniel, PREUSS, Mary Lai, PRUESSE, Elmar, RASMUSSEN, Lasse Buur, RIVERS, Adam, ROBESON, Michael S., ROSENTHAL, Patrick, SEGATA, Nicola, SHAFFER, Michael, SHIFFER, Arron, SINHA, Rashmi, SONG, Se Jin, SPEAR, John R., SWAFFORD, Austin D., THOMPSON, Luke R., TORRES, Pedro J., TRINH, Pauline, TRIPATHI, Anupriya, TURNBAUGH, Peter J., UL-HASAN, Sabah, VAN DER HOOFT, Justin J. J., VARGAS, Fernando, VÁZQUEZ-BAEZA, Yoshiki, VOGTMANN, Emily, VON HIPPEL, Max, WALTERS, William, WAN, Yunhu, WANG, Mingxun, WARREN, Jonathan, WEBER, Kyle C., WILLIAMSON, Charles H. D., WILLIS, Amy D., XU, Zhenjiang Zech, ZANEVELD, Jesse R., ZHANG, Yilong, ZHU, Qiyun, KNIGHT, Rob and CAPORASO, J. Gregory, 2019. Reproducible, interactive, scalable and extensible microbiome data science using QIIME 2. *Nature Biotechnology*. Online. August 2019. Vol. 37, no. 8, p. 852–857. DOI 10.1038/s41587-019-0209-9. [Accessed 11 May 2024].

CHAN, Carmen Ka-Man, FANG, James Kar-Hei, FEI, Bin and KAN, Chi-Wai, 2023. Microfibres Release from Textile Industry Wastewater Effluents Are Underestimated: Mitigation Actions That Need to Be Prioritised. *Fibers*. Online. December 2023. Vol. 11, no. 12, p. 105. DOI 10.3390/fib11120105. [Accessed 8 May 2024].

CHUNG, Chinkap, LEE, Myunghee and CHOE, Eun Kyung, 2004. Characterization of cotton fabric scouring by FT-IR ATR spectroscopy. *Carbohydrate Polymers*. Online. 7 December 2004. Vol. 58, no. 4, p. 417–420. DOI 10.1016/j.carbpol.2004.08.005. [Accessed 12 May 2024].

CYPROWSKI, Marcin, STOBNICKA-KUPIEC, Agata, ŁAWNICZEK-WAŁCZYK, Anna, BAKAL-KIJEK, Aleksandra, GOŁOFIT-SZYMCZAK, Małgorzata and GÓRNY, Rafał L., 2018. Anaerobic bacteria in wastewater treatment plant. . Online. 1 July 2018. Vol. 91, no. 5, p. 571–579. DOI 10.1007/s00420-018-1307-6. [Accessed 27 April 2024].

DAIMS, Holger, TAYLOR, Michael W. and WAGNER, Michael, 2006. Wastewater treatment: a model system for microbial ecology. *Trends in Biotechnology*. Online. 1 November 2006. Vol. 24, no. 11, p. 483–489. DOI 10.1016/j.tibtech.2006.09.002. [Accessed 27 April 2024].

DE FALCO, Francesca, DI PACE, Emilia, COCCA, Mariacristina and AVELLA, Maurizio, 2019. The contribution of washing processes of synthetic clothes to microplastic pollution. *Scientific Reports*. Online. 29 April 2019. Vol. 9, no. 1, p. 6633. DOI 10.1038/s41598-019-43023-x. [Accessed 11 May 2024].

DEITEX, [no date]. Microfiber. *Decitex | Smart Textiles*. Online. Available from: <https://www.decitex.com/en/microfiber> [Accessed 12 May 2024].

DEROMBISE, Guillaume, VOUYOVITCH VAN SCHOORS, Laëtitia, MESSOU, Marie-Fleur and DAVIES, Peter, 2010. Influence of finish treatment on the durability of aramid fibers aged under an alkaline environment. *Journal of Applied Polymer Science*. Online. 2010. Vol. 117, no. 2, p. 888–898. DOI 10.1002/app.31534. [Accessed 12 May 2024].

DIMKIĆ, Ivica, ČOPIĆ, Milica, PETROVIĆ, Marija, STUPAR, Miloš, SAVKOVIĆ, Željko, KNEŽEVIĆ, Aleksandar, SUBAKOV SIMIĆ, Gordana, LJALJEVIĆ GRBIĆ, Milica and UNKOVIĆ, Nikola, 2023. Bacteriobiota of the Cave Church of Sts. Peter and Paul in Serbia—Culturable and Non-Culturable Communities’ Assessment in the Bioconservation Potential of a Peculiar Fresco Painting. *International Journal of Molecular Sciences*. Online. 5 January 2023. Vol. 24, no. 2, p. 1016. DOI 10.3390/ijms24021016. [Accessed 11 May 2024].

EUROPEAN ENVIRONMENT AGENCY., 2022. Microplastics from textiles: towards a circular economy for textiles in Europe. *Briefing*. Online. 10 February 2022. Vol. 2021, no. 16. DOI 10.2800/863646. [Accessed 8 May 2024].

GOONVEAN FIBRES, 2024. Products & Services. *Goonvean Fibres*. Online. 2024. Available from: <https://goonveanfibres.com/products-services/> [Accessed 11 May 2024].

LIU, Jianli, LIU, Qiang, AN, Lihui, WANG, Ming, YANG, Qingbo, ZHU, Bo, DING, Jiannan, YE, Chuanyu and XU, Yuyao, 2022. Microfiber Pollution in the Earth System. *Reviews of Environmental Contamination and Toxicology*. Online. 2022. Vol. 260, no. 1, p. 13. DOI 10.1007/s44169-022-00015-9. [Accessed 11 May 2024].

LIZA, Afroza Akter, ASHRAFY, Asifa, ISLAM, Md. Nazrul, BILLAH, Md. Morsaline, AR-AFAT, Shaikh Tareq, RAHMAN, Md. Moshiur, KARIM, Md. Rezaul, HASAN, Md. Mehedi, PROMIE, Ahsan Rajib and RAHMAN, Sheikh Mustafizur, 2024. Microplastic pollution: a review of techniques to identify microplastics and their threats to the aquatic ecosystem. *Environmental Monitoring and Assessment*. Online. 20 February 2024. Vol. 196, no. 3, p. 285. DOI 10.1007/s10661-024-12441-4. [Accessed 27 April 2024].

MAHLTIG, Boris, 2021. High-Performance Fibres – A Review of Properties and IR-Spectra. *Tekstilec*. Online. 28 March 2021. Vol. 64, no. 2, p. 96–118. DOI 10.14502/Tekstilec2021.64.96-118. [Accessed 12 May 2024].

MP BIOMEDICALS, 2021. FastDNA™ Spin Kit for Soil DNA Extraction. . Online. May 2021. Available from: <https://www.mpbio.com/116560000-fastdna-spin-kit-for-soil-samp-cf> [Accessed 14 May 2024]. Cat. No. 116560200/116560300

NAM, Sunghyun, SLOPEK, Ryan, WOLF, Duane, WARNOCK, Mary, CONDON, Brian D., SAWHNEY, Paul, GBUR, Edward, REYNOLDS, Michael and ALLEN, Chuck, 2015. Comparison of biodegradation of low-weight hydroentangled raw cotton nonwoven fabric and that of commonly used disposable nonwoven fabrics in aerobic Captina silt loam soil. *Textile Research Journal*. Online. 12 May 2015. DOI 10.1177/0040517514551468. [Accessed 12 May 2024].

NAPPER, Imogen E. and THOMPSON, Richard C., 2016. Release of synthetic microplastic plastic fibres from domestic washing machines: Effects of fabric type and washing conditions. *Marine Pollution Bulletin*. Online. 15 November 2016. Vol. 112, no. 1, p. 39–45. DOI 10.1016/j.marpolbul.2016.09.025. [Accessed 27 April 2024].

NGUYEN, Nhung H. A., ŠPÁNEK, Roman, KASALICKÝ, Vojtěch, RIBAS, David, VLKOVÁ, Denisa, ŘEHÁKOVÁ, Hana, KEJZLAR, Pavel and ŠEVCŮ, Alena, 2018. Different effects of nano-scale and micro-scale zero-valent iron particles on planktonic microorganisms from natural reservoir water. *Environmental Science: Nano*. Online. 17 May 2018. Vol. 5, no. 5, p. 1117–1129. DOI 10.1039/C7EN01120B. [Accessed 11 May 2024].

NI, Bing-Jie, YU, Han-Qing and ZENG, Raymond J., 2015. Understanding the Microbial Internal Storage Turnover in Wastewater Treatment: Retrospect, Prospect, and Challenge. *Critical Reviews in Environmental Science and Technology*. Online. 19 March 2015. Vol. 45, no. 6, p. 591–612. DOI 10.1080/10643389.2013.876525. [Accessed 27 April 2024].

PUÓN-PELÁEZ, Xiao-Haitzi Daniel, MCEWAN, Neil Ross, ÁLVAREZ-MARTÍNEZ, Roberto Carlos, MARISCAL-LANDÍN, Gerardo, NAVA-MORALES, Gerardo Manuel, MOSQUEDA, Juan and OLVERA-RAMÍREZ, Andrea Margarita, 2022. Effect of Feeding Insoluble Fiber on the Microbiota and Metabolites of the Caecum and Feces of Rabbits Recovering from Epizootic Rabbit Enteropathy Relative to Non-Infected Rabbits. *Pathogens*. Online. May 2022. Vol. 11, no. 5, p. 571. DOI 10.3390/pathogens11050571. [Accessed 11 May 2024].

RAMASAMY, Rathinamoorthy, ARAGAW, Tadele Assefa and BALASARASWATHI SUBRAMANIAN, Raja, 2022. Wastewater treatment plant effluent and microfiber pollution: focus on industry-specific wastewater. *Environmental Science and Pollution Research*. Online. 1 July 2022. Vol. 29, no. 34, p. 51211–51233. DOI 10.1007/s11356-022-20930-7. [Accessed 8 May 2024].

RANDHAWA, Jatinder Singh, 2023. Advanced analytical techniques for microplastics in the environment: a review. *Bulletin of the National Research Centre*. Online. 5 December 2023. Vol. 47, no. 1, p. 174. DOI 10.1186/s42269-023-01148-0. [Accessed 8 May 2024].

ROCHA-SANTOS, Teresa, COSTA, Monica F. and MOUNEYRAC, Catherine (eds.), 2022. *Handbook of Microplastics in the Environment*. Online. Cham: Springer International Publishing. ISBN 978-3-030-39040-2. [Accessed 18 January 2024].

SILVA, Ana B., BASTOS, Ana S., JUSTINO, Celine I. L., DA COSTA, João P., DUARTE, Armando C. and ROCHA-SANTOS, Teresa A. P., 2018. Microplastics in the environment: Challenges in analytical chemistry - A review. *Analytica Chimica Acta*. Online. 9 August 2018. Vol. 1017, p. 1–19. DOI 10.1016/j.aca.2018.02.043. [Accessed 27 April 2024].

SILVA, R. C. Lima da, ALVES, C., NASCIMENTO, J. H., NEVES, J. R. O. and TEIXEIRA, V., 2012. Surface Modification of Polyester Fabric by Non-Thermal Plasma Treatment. *Journal of Physics: Conference Series*. Online. December 2012. Vol. 406, no. 1, p. 012017. DOI 10.1088/1742-6596/406/1/012017. [Accessed 12 May 2024].

SILVESTRI, Daniele, WACŁAWEK, Stanisław, SOBEL, Bartłomiej, TORRES-MENDIETA, Rafael, NOVOTNÝ, Vít, NGUYEN, Nhung H. A., ŠEVČŮ, Alena, PADIL, Vinod V. T., MÜLLEROVÁ, Jana, STUHLÍK, Martin, PAPINI, Marco Petrangeli, ČERNÍK, Miroslav and VARMA, Rajender S., 2018. A poly(3-hydroxybutyrate)–chitosan polymer conjugate for the synthesis of safer gold nanoparticles and their applications. *Green Chemistry*. Online. 29 October 2018. Vol. 20, no. 21, p. 4975–4982. DOI 10.1039/C8GC02495B. [Accessed 11 May 2024].

SÜLAR, Vildan and DEVRIM, Gökberk, 2019. Biodegradation Behaviour of Different Textile Fibres: Visual, Morphological, Structural Properties and Soil Analyses. *Fibres & Textiles in Eastern Europe*. Online. 2019. No. 1 (133), p. 100–111. Available from: <https://bibliotekanauki.pl/articles/232655> [Accessed 12 May 2024].

SYBERG, Kristian, NIELSEN, Maria Bille, OTURAI, Nikoline B., CLAUSEN, Lauge Peter Westergaard, RAMOS, Tiffany Marilou and HANSEN, Steffen Foss, 2022. Circular economy and reduction of micro(nano)plastics contamination. *Journal of Hazardous Materials Advances*. Online. 1 February 2022. Vol. 5, p. 100044. DOI 10.1016/j.hazadv.2022.100044. [Accessed 11 February 2024].

TAKABATAKE, H., SATOH, H., MINO, T. and MATSUO, T., 2002. PHA (polyhydroxyalkanoate) production potential of activated sludge treating wastewater. *Water Science and Technology*. Online. 1 June 2002. Vol. 45, no. 12, p. 119–126. DOI 10.2166/wst.2002.0417. [Accessed 27 April 2024].

TALVITIE, Julia, MIKOLA, Anna, SETÄLÄ, Outi, HEINONEN, Mari and KOISTINEN, Arto, 2017. How well is microlitter purified from wastewater? – A detailed study on the step-wise removal of microlitter in a tertiary level wastewater treatment plant. *Water Research*. Online. 1 February 2017. Vol. 109, p. 164–172. DOI 10.1016/j.watres.2016.11.046. [Accessed 27 April 2024].

THERMOFISHER, 2021. Qubit 4 Assays Quick Reference. *ThermoFisher SCIENTIFIC*. Online. 12 March 2021. Available from: [https://www.thermofisher.com/document-connect/document-connect.html?url=https://assets.thermofisher.com/TFS-Assets/BID/manuals/MAN0017210\\_Qubit\\_4\\_Assays\\_QR.pdf&title=UXVpY2sIMjUyMFJlZmVyZW5jZSUzQSUyNTIwUXVlXQIMjUyMDQIMjUyMEFzc2F5cw==](https://www.thermofisher.com/document-connect/document-connect.html?url=https://assets.thermofisher.com/TFS-Assets/BID/manuals/MAN0017210_Qubit_4_Assays_QR.pdf&title=UXVpY2sIMjUyMFJlZmVyZW5jZSUzQSUyNTIwUXVlXQIMjUyMDQIMjUyMEFzc2F5cw==) [Accessed 14 May 2024]. Pub. No. MAN0017210 C.0

WEIS, Judith S., FALCO, Francesca De and COCCA, Mariacristina (eds.), 2022. *Polluting Textiles: The Problem with Microfibres*. London: Routledge. ISBN 978-1-00-316538-5.

WERNER, Anja, SCHÄFER, Simon, GLEUSSNER, Nina, NIMMERJAHN, Falk and WINKLER, Thomas H., 2022. Determining immunoglobulin-specific B cell receptor repertoire of murine splenocytes by next-generation sequencing. *STAR Protocols*. Online. 17 June 2022. Vol. 3, no. 2, p. 101277. DOI 10.1016/j.xpro.2022.101277. [Accessed 16 April 2024].

WU, Linwei, NING, Daliang, ZHANG, Bing, LI, Yong, ZHANG, Ping, SHAN, Xiaoyu, ZHANG, Qiuting, BROWN, Mathew Robert, LI, Zhenxin, VAN NOSTRAND, Joy D., LING, Fangqiong, XIAO, Naijia, ZHANG, Ya, VIERHEILIG, Julia, WELLS, George F., YANG, Yunfeng, DENG, Ye, TU, Qichao, WANG, Aijie, ZHANG, Tong, HE, Zhili, KELLER, Jurg, NIELSEN, Per H., ALVAREZ, Pedro J. J., CRIDDLE, Craig S., WAGNER, Michael, TIEDJE, James M., HE, Qiang, CURTIS, Thomas P., STAHL, David A., ALVAREZ-COHEN, Lisa, RITTMANN, Bruce E., WEN, Xianghua and ZHOU, Jizhong, 2019. Global diversity and biogeography of bacterial communities in wastewater treatment plants. *Nature Microbiology*. Online. July 2019. Vol. 4, no. 7, p. 1183–1195. DOI 10.1038/s41564-019-0426-5. [Accessed 27 April 2024].

WU, Xiaowei, ZHAO, Xiaoli, CHEN, Rouzheng, LIU, Peng, LIANG, Weigang, WANG, Junyu, TENG, Miaomiao, WANG, Xia and GAO, Shixiang, 2022. Wastewater treatment plants act as essential sources of microplastic formation in aquatic environments: A critical review. *Water Research*. Online. 1 August 2022. Vol. 221, p. 118825. DOI 10.1016/j.watres.2022.118825. [Accessed 27 April 2024].

ZHANG, Ya-Qi, LYKAKI, Marianna, ALRAJOULA, Mohammad Taher, MARKIEWICZ, Marta, KRAAS, Caroline, KOLBE, Sabrina, KLINKHAMMER, Kristina, RABE, Maike, KLAUER, Robert, BENDT, Ellen and STOLTE, Stefan, 2021. Microplastics from textile origin – emission and reduction measures. *Green Chemistry*. Online. 2 August 2021. Vol. 23, no. 15, p. 5247–5271. DOI 10.1039/D1GC01589C. [Accessed 11 February 2024].

ZHU, Chao, CHEN, Jianmin, WANG, Xinfeng, LI, Jiarong, WEI, Min, XU, Caihong, XU, Xianmang, DING, Aijun and JEFFREY L. COLLETT, Jr, 2018. Chemical Composition and Bacterial Community in Size-Resolved Cloud Water at the Summit of Mt. Tai, China. *Aerosol and Air Quality Research*. Online. 2018. Vol. 18, no. 1, p. 1–14. DOI 10.4209/aaqr.2016.11.0493. [Accessed 30 April 2024].